Title

The differential regulation of placenta trophoblast bisphosphoglycerate mutase in fetal growth restriction: preclinical study in mice and observational histological study of human placenta.

Authors

Sima Stroganov[1], Talia Harris[1], Liat Fellus-Alyagor[1], Lital Ben Moyal[1], Romina Plitman Mayo[1], Ofra Golani[1], Alexander Brandis[1], Tevie Mehlman[1], Michal Kovo[2], Tal Biron-Shental[2], Nava Dekel[1], Michal Neeman[1]

1 Weizmann Institute of Science, Israel

2 Meir Medical Center; Tel Aviv University, School of Medicine, Israel

Abstract

Background Fetal growth restriction (FGR) is a pregnancy complication in which a newborn fails to achieve its growth potential, increasing the risk of perinatal morbidity and mortality. Chronic maternal gestational hypoxia, as well as placental insufficiency are associated with increased FGR incidence; however, the molecular mechanisms underlying FGR remain unknown.

Methods In a case control study of murine and human control and FGR placentae, we implied MR imaging, IHC and metabolomics to assess the levels of BPGM and 2,3 BPG to elucidate the impact of maternal gestational hypoxia, and the molecular mechanisms underlying human FGR.

Results We show that murine acute and chronic gestational hypoxia recapitulates FGR phenotype and affects placental structure and morphology. Gestational hypoxia decreased labyrinth area, increased the incidence of red blood cells (RBCs) in the labyrinth while expanding the placental spiral arteries (SpA) diameter. Hypoxic placentae exhibited higher hemoglobin-oxygen affinity compared to the control. Placental abundance of bisphosphoglycerate mutase (BPGM) was upregulated in the syncytiotrophoblast and spiral artery trophoblast cells (SpA TGCs) in the murine gestational hypoxia groups compared to the control. In contrast, human FGR placentae exhibited reduced BPGM levels in the syncytiotrophoblast layer compared to placentae from healthy uncomplicated pregnancies. Levels of 2,3 BPG, the product of BPGM, were lower in cord serum of human FGR placentae compared to control. Polar expression of

BPGM, was found in both human and mouse placentae syncytiotrophoblast, with higher expression facing the maternal circulation. Moreover, in the murine SpA TGCs expression of BPGM was concentrated exclusively in the apical cell side, in direct proximity to the maternal circulation.

Conclusions This study suggests a possible involvement of placental BPGM in maternal-fetal oxygen transfer, and in the pathophysiology of FGR.

Funding This work was supported by the Weizmann - Ichilov (Tel Aviv Sourasky Medical Center) Collaborative Grant in Biomedical Research (to MN) and by the Israel Science Foundation KillCorona grant 3777/19 (to MN, MK).

Introduction

The placenta is a transient organ, crucial for the growth and development of the fetus during gestation[12]. The placenta provides the interface between the maternal and fetal circulation, mediating gas and metabolic exchange along with fetal waste disposal[3]. Abnormalities in placental growth, structure, and function are associated with gestational complications such as fetal growth restriction (FGR)[45], which is defined as the failure of the fetus to reach its growth potential[6]. The clinical definition of FGR is fetal weight below the 10th percentile of predicted fetal weight for gestational age[7]. FGR affects approximately 10-15% of pregnancies, increasing the risk of perinatal morbidity and mortality[6]. Long-term complications of FGR include poor postnatal development and are associated with multiple adverse health outcomes including respiratory, metabolic and cardiovascular deficits [89].

There are numerous etiologies for FGR, some of which are related to fetal genetic aberrations or malformations, others related to placental or umbilical malformation, or also to maternal infections or diseases. Maternal anemia, smoking, high altitude residency, as well as placental and umbilical cord anomalies, are all associated with restricted placental and fetal oxygen availability[10]. Interestingly, about 40 percent of all FGR cases are idiopathic[11], with no identifiable cause, which might hint on possible biological pre disposition factors that contribute to FGR development by creating an hypoxic placental or embryo environment. However, the

molecular mechanisms that provoke and contribute to this pregnancy complication have yet to be elucidated.

One of the key placental functions is the transfer of oxygen from the mother to the fetus[12], and inefficient oxygen transport and availability is detrimental for placental and embryonic development[1314]. Late-gestation hypoxia results in utero-placental vascular adaptations, such as capillary expansion, thinning of the inter-haemal membrane and increased radial artery diameters[15]. Moreover, there is substantial evidence that late-gestation exposure to hypoxic environment alters placental structure and functionality[1617]. *In-vitro* studies on human placental samples under acute reduction of oxygen tension induced direct placental vasoconstriction[18]. Placental oxygen transport depends on Hemoglobin (Hb), which is responsible for carrying and mediating oxygen transfer in mammalian organisms[19]. BOLD contrast MR imaging is a powerful tool that utilizes hemoglobin as an endogenous reporter molecule to assess oxygen-hemoglobin affinity[20]. Previous MR studies have shown altered placental oxygen-Hb affinity following exposure to hypoxia[21]. However, limited information is available on how placental structure and function is altered in chronic gestational hypoxia that commences at the onset of gestation.

The most significant allosteric effectors of Hb are organic phosphates, specifically 2,3 BPG, which is produced by the BPGM enzyme in a unique side reaction of glycolysis, known as the Luebering-Rapoport pathway[22]. 2,3 BPG plays a key role in delivering O_2 to tissues by binding to and stabilizing deoxy-hemoglobin, thus leading to the release of oxygen from the Hb unit[2324]. During gestation, fetal hemoglobin (HbF) is the dominant form of Hb present in the fetus, comprised of α and γ subunits[25]. During late gestation, the γ subunit is gradually replaced by the adult β subunit[25]. HbF has a higher affinity to oxygen compared to the adult Hb, caused by a structural difference, which leads to a weakened ability to bind 2,3 BPG[262728]. The transfer of oxygen from maternal to fetal Hb is facilitated by the higher affinity of maternal Hb to 2,3 BPG[24]. Remarkably, BPGM expression is specifically restricted to erythrocytes and the syncytiotrophoblast of the placenta, a multinucleated layer that mediates transport of oxygen and nutrients from the mother to the fetus[29]. In a study that used *igf2*$^{+/-}$ knockout mice as a model of FGR, BPGM expression in the placental labyrinth was lower compared to wild type placentae[30]. However, scarce information is available on the role of this enzyme during gestation.

We report here that placental BPGM expression pattern is consistent with a role in adaptation of the placenta to gestational hypoxia, facilitating the transfer of oxygen from maternal to fetal circulation. Here we show that gestational hypoxia augments placental BPGM expression in mice, while in human FGR placentae of unknown etiology BPGM expression is suppressed.

Graphical abstract

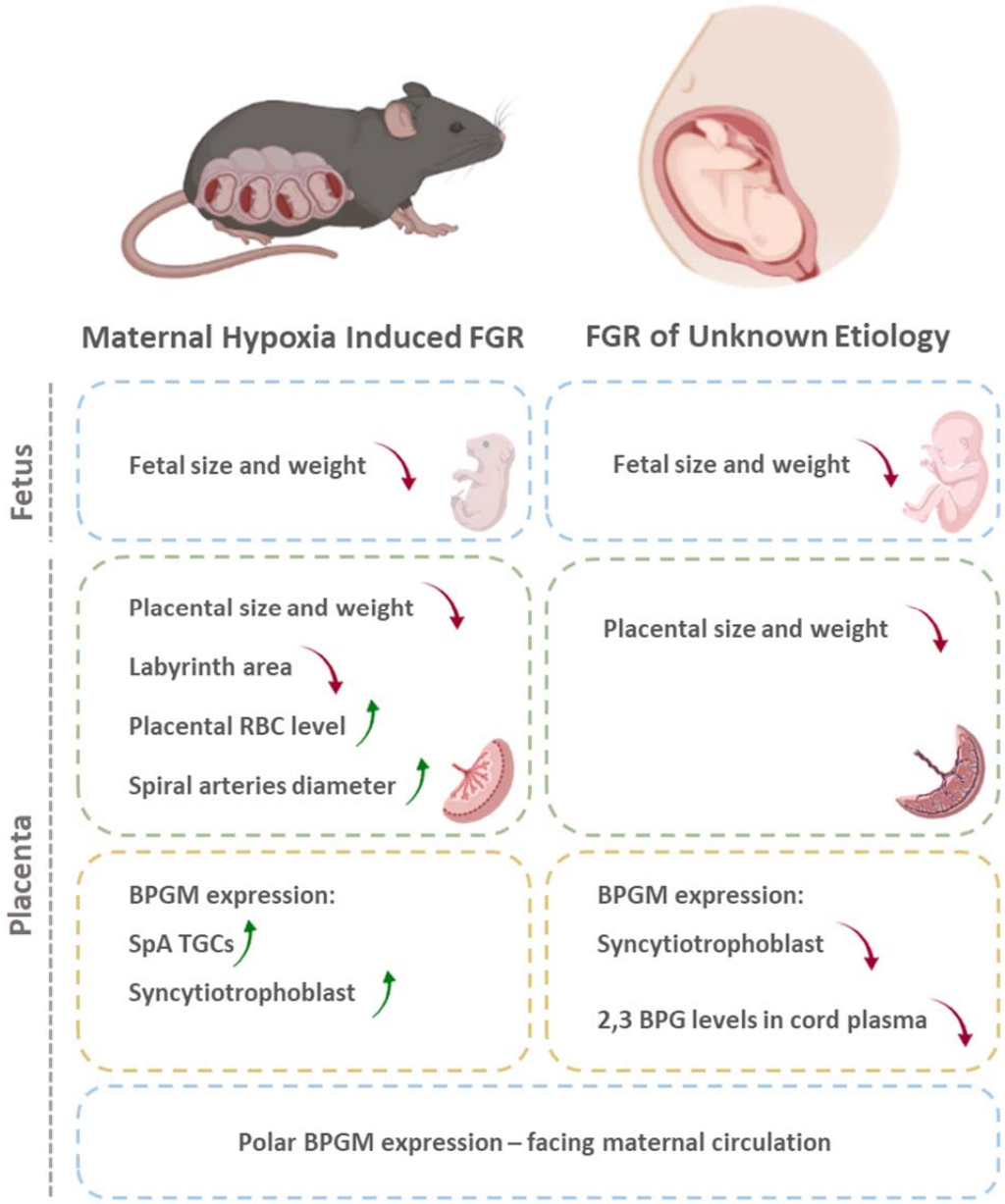

103

104

105

106

107

108 **Results**

Gestational Hypoxia Affects Maternal Hematological Parameters and Recapitulates FGR Phenotype

Maternal hypoxia during pregnancy increases the risk of FGR [3132]. To gain an understanding of BPGM contribution to placental development and functionality following maternal hypoxia, we established a murine model of acute and chronic gestational hypoxia. Increased erythropoiesis is the best-known physiological response to chronic hypoxia[33]. Exposure to chronic hypoxia during gestation significantly elevated maternal blood hematocrit and Hb levels (by 4.9±1.62 %PCV, *P*=0.0243 and by 1.693±0.54 g/DL, *P*=0.0217 respectively, Figure 1 A, B) relative to the control group. Both acute and chronic gestational hypoxia resulted in a significant increase in blood acidity, presented by a decrease in pH values (*P*=0.0032 acute hypoxia versus control, *P*=0.0462 chronic hypoxia versus control, Figure 1 C).

Gestational acute and chronic hypoxia did not affect litter size (Figure 1 D). Thereafter, the effect of gestational hypoxia on placental and fetal weight was assessed. A significant decrease in placental weight was observed in both gestational hypoxia groups and in fetuses of the chronic hypoxia group (acute hypoxia placentae by 15.03±4.2 mg, *P*=0.0068,; chronic hypoxia placentae by 11.84±4.06 mg, *P*=0.0258 and fetuses by 50.24±18.11 mg, *P*=0.0343, Figure 1 E- G) when compared to the control group. To further examine the weight differences, the percent of small, average or large for gestational age (SGA, AGA and LGA respectively) fetuses and placentae were compared to the control group. The results show that in the acute hypoxia group 45% of the fetuses are SGA and only 2% LGA, whereas in the chronic hypoxia group 50% of the fetuses are SGA and only 5% LGA (Figure 1 H). Furthermore, the placentae exhibited a similar phenotype, where in the acute hypoxia group 35% of the placentae are SGA and none were LGA, whereas in the chronic hypoxia group 21% of the placentae were SGA and only 1.6% LGA (Figure 2 I).

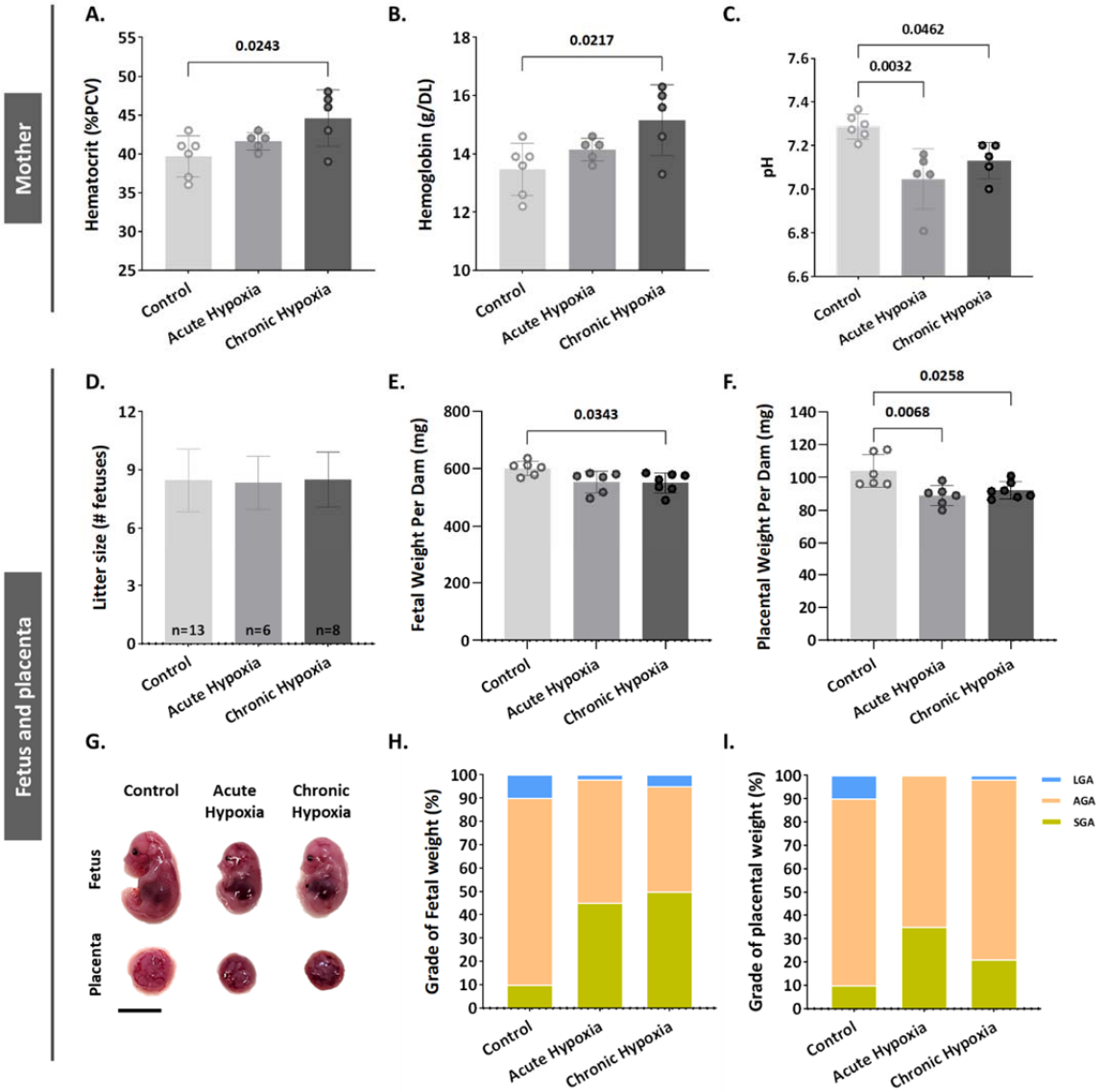

Figure 1. Gestational hypoxia elevates maternal hemoglobin, hematocrit and blood acidity, and recapitulates FGR phenotype. (**A-B**) Graphs showing hematocrit and hemoglobin levels in maternal venous blood. (**C**) Graph shows pH levels in maternal venous blood. (**D-F**) Graphs showing litter size, fetal weight and placental weight. (**G**) Representative picture of fetuses and placentae (E16.5) from control and gestational hypoxia groups. (**H-I**) Analysis of the percentage of small for gestational age (SGA, weight less than the 10th percentile) fetuses and placentae, large for gestational age (LGA, weight greater than the 90th percentile) fetuses and placentae, and appropriate for gestational age (AGA, weight between the 10th and 90th percentiles) fetuses and placentae at E16.5. Scale bars: 1 cm. Data displayed as mean ± SD and are from 49-62 fetuses and placentae from 6-7 dams per group (8–9 conceptuses per litter used). Ordinary one-way ANOVA test was used for statistical analysis.

147 **Gestational Hypoxia Alters Placental Morphology**

148 To determine whether the gestational hypoxia leads to structural changes of the placenta, the
149 placental morphology, and particularly the labyrinth area were examined. The labyrinth area of
150 the chronic and gestational hypoxia-exposed mice was significantly smaller (P=0.0001 for the
151 acute and P=0.0003 for the chronic hypoxia groups, Figure 2 A, B) compared to the control
152 group. Furthermore, the diameter of the placental spiral arteries (SpA) was enlarged in the
153 chronic hypoxia group (Figure 2 C, D, P=0.0420) as compared to the control. In addition, in both
154 acute and chronic hypoxia groups the density of RBCs in the labyrinth were significantly higher
155 (P=0.0008 for the acute and P=0.007 for the chronic hypoxia groups, Figure 2 E, F) compared to
156 the control.

157

158

159

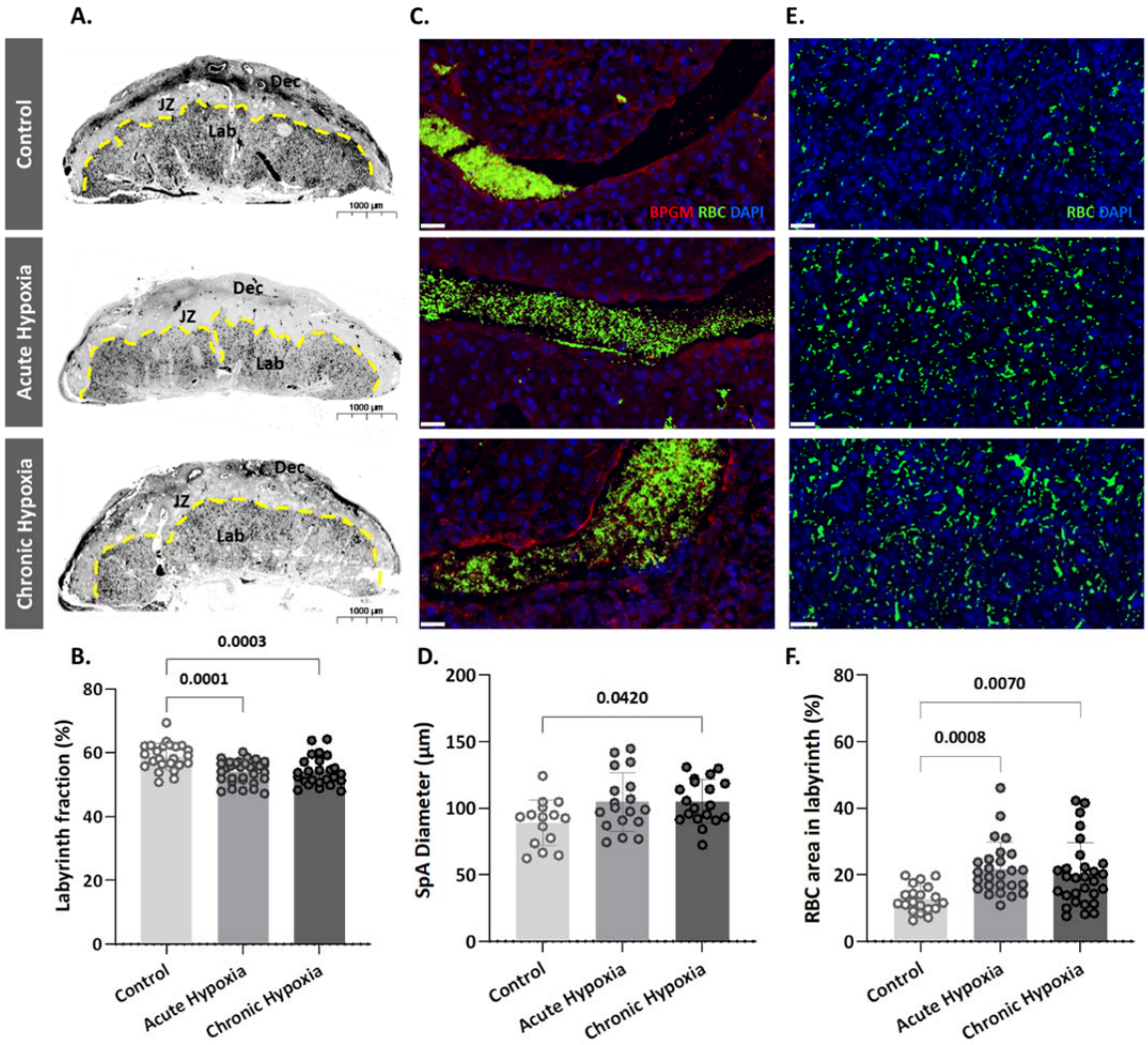

Figure 2. Maternal hypoxia during gestation results in enlarged spiral arteries, increased RBC levels and decreased placental labyrinth area. (**A, B**) Placentae of hypoxic chamber groups have significantly smaller labyrinth area in comparison to the control group.(**C ,D, E, F**) Placentae of hypoxic chamber groups display enlarged spiral arteries and increased RBC levels in the labyrinth. Scale bars: 40 µm. Data are from 3 control, 4 chronic hypoxia and 4 acute hypoxia dams, 5-7 placentae per dam and presented as mean ± SD values. Ordinary one-way ANOVA test was used for statistical analysis.

R2* Maps Reveals Maternal, But Not Placental or Fetal changes in deoxygenated hemoglobin concentration

As shown above, gestational hypoxia alters placental structure. To determine whether and how gestational hypoxia affects placental functionality, the pregnant dams (E16.5) were subjected to hyperoxia-hypoxia challenge during ultra-high field (15.2T) MR imaging (Appendix, video 1, 2, 3). R2* values were calculated at each oxygen challenge for the maternal aorta, vena cava and liver (Figure 3 A-D, Appendix Figure S1), and for the placenta, embryo heart, liver and aorta (Figure 3 E-H). The maternal aorta R2* levels from the chronic hypoxia group were significantly higher ($P=0.0376$, Figure 3 A) than in the control group, when subjected to 10% O_2. However, no differences were observed in maternal liver and vena cava when compared to that of the control group (Figure 4 B, D). Similarly, no differences were observed in the R2* of embryonic tissues (aorta, heart and liver), nor in the placenta, when comparing the hypoxic groups to the control (Figure 4 E-H). To better understand the signal distribution in the different placental regions, the R2* maps of the placentae were further analyzed. Interestingly no significant differences in the spatial distribution of R2* were observed in the placentae of hypoxic and control groups (Figure 3 J).

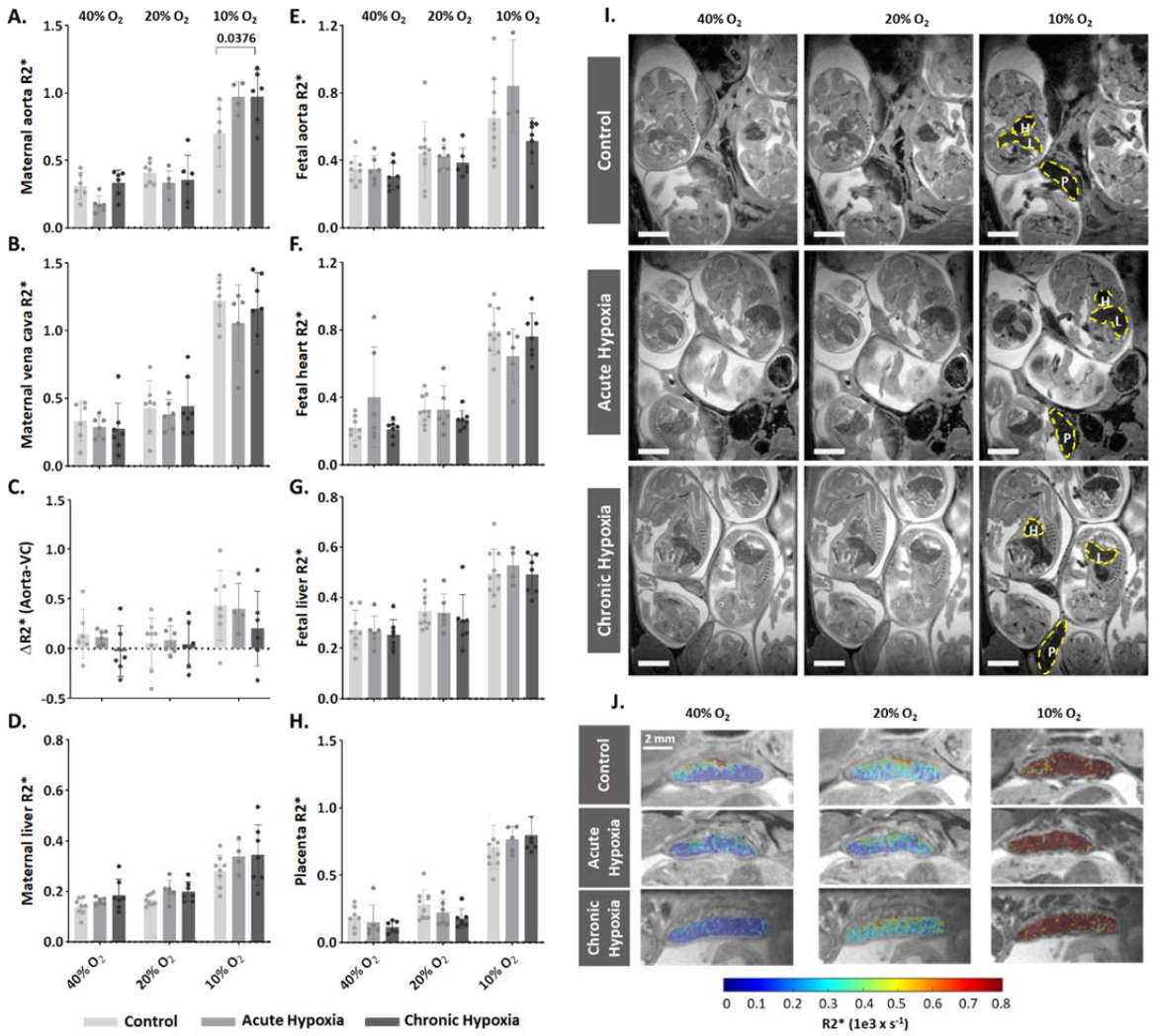

Figure 3. Effects of maternal hypoxia during gestation on R2* values following hyperoxia-hypoxia challenge. (**A-H**) Graphs show that hypoxic challenge results in elevation in R2* values in maternal aortas of chronic hypoxia chamber group, while no differences are observed in the respective placentae and fetuses. (**I**) Representative R2* images of control and hypoxic chamber group show several fetuses and their placenta (P), heart (H) and liver (L). Scale bars: 0.5 cm. (**J**) Representative R2* maps inside the placenta of control, acute hypoxia (AH) and chronic hypoxia (CH) chamber groups at E16.5 show distribution of R2* values following hyperoxia-hypoxia challenge. Data are from 8 control, 6 acute hypoxia and 7 chronic hypoxia per dams presented as mean ± SD values. R2* values of embryonic tissues and placentae are calculated as the median per mother, 5-8 embryos per each mother. Ordinary one-way ANOVA test was used for statistical analysis.

207

208 **BPGM is Upregulated in Placental Cells Following Gestational Hypoxia**

209 Our present findings revealed structural changes in placentae from hypoxic mothers, however
210 functional MRI experiments demonstrated that placental deoxyhemoglobin concentrations are
211 similar to the control group. BPGM expression was previously observed in human placental
212 syncytiotrophoblast cells from healthy pregnancies[29]. Therefore, we inspected the expression of
213 BPGM in the labyrinth of the gestational hypoxia FGR murine model compared to the control.
214 Significant differences were observed in the syncytiotrophoblast BPGM expression between the
215 hypoxic and control placentae (Figure 4 A, C). Although BPGM expression has only been
216 reported in the syncytiotrophoblast, we also inspected the BPGM expression in other placental
217 cells that come in direct contact with maternal blood. BPGM expression was found also in the
218 spiral artery trophoblast cells (SpA TGCs), an expression that is upregulated following acute and
219 chronic maternal hypoxia (Figure 4 D); moreover, SpA TGCs BPGM expression was found to be
220 polar and concentrated in the apical cell side facing the arterial lumen (Figure 4 B).

221

222

223

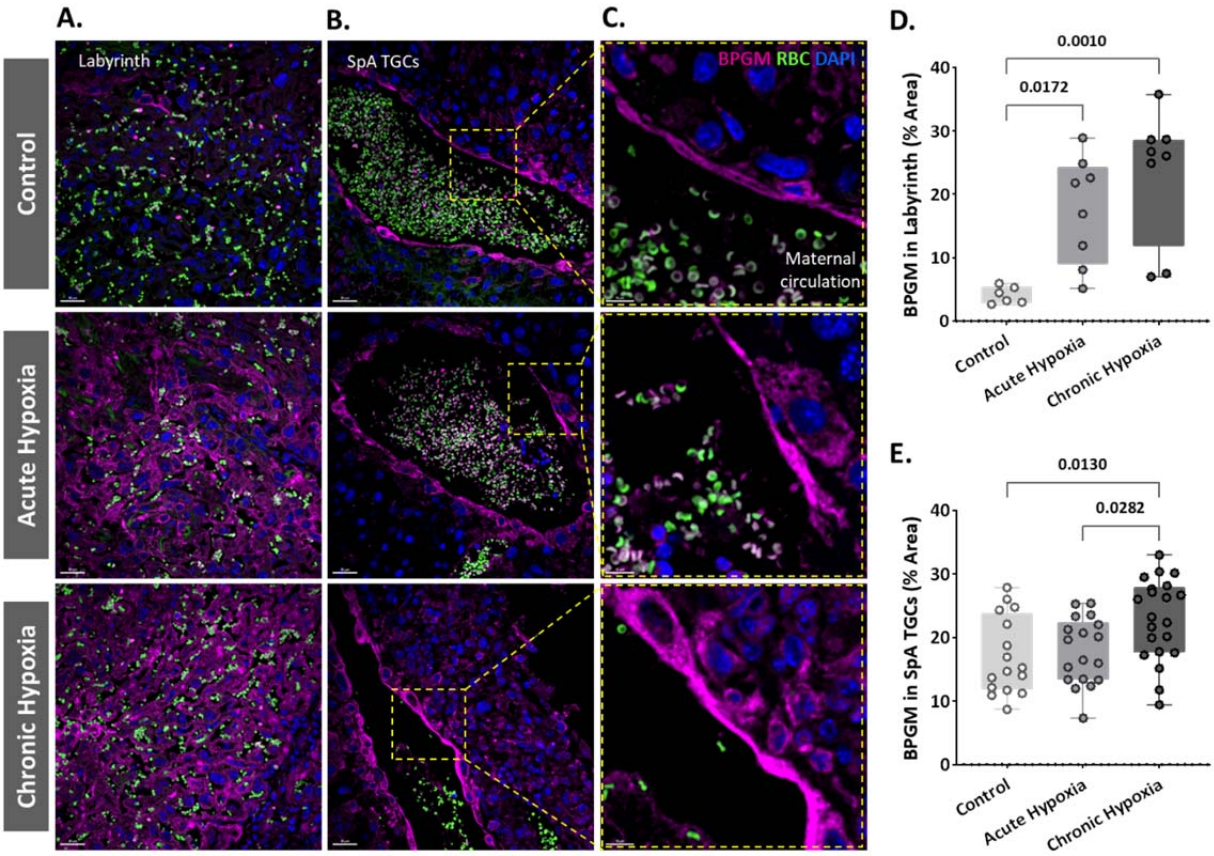

Figure 4. Maternal hypoxia during gestation results in elevated placental BPGM expression levels. (**A**,**D**) Representative images and quantification of BPGM expression in the placental labyrinth at E16.5 of control and hypoxic chamber groups. Scale bars: 30 µm (**B**,**C**,**E**) Trophoblast cells lining the arteries show an increase of BPGM expression in chronic hypoxia group. The expression of BPGM is restricted to the apical trophoblast cell side facing the arterial lumen. Scale bars: 30 µm (B), 10 µm (C). Data are from 3 control, 4 chronic hypoxia and 4 acute hypoxia dams, 2-3 placentae per group and presented as mean ± SD values. Ordinary one-way ANOVA test was used for statistical analysis.

BPGM expression is Downregulated in Human FGR placentae

An upregulation of syncytiotrophoblast and SpA TGCs BPGM levels was detected in the murine gestational hypoxia placentae. Therefore, to determine whether BPGM expression is also altered in human placental syncytiotrophoblast cells of pregnancies complicated by FGR, human placentae from healthy and FGR-complicated third-trimester pregnancies were examined. Seventeen samples collected from Meir and Wolfson Medical Centers were selected from 236 deliveries ,following childbirth and classified into two groups: FGR complicated pregnancies and matched control deliveries (Table 1 and Figure 5). Clinical characteristics and neonatal outcomes are provided in Table 1. Clinical parameters did not differ among the groups, except for birthweight, which was significantly lower in the FGR group, as compared with the control (Unpaired t-test; P = 0.0004). A downregulation of syncytiotrophoblast cells BPGM levels was observed in the FGR placentae (Figure 6 C). No differences were observed in 2,3 BPG levels in maternal plasma analyzed by mass spectrometry (Figure 6 D, E). However, the results demonstrated a significant reduction of 2,3 BPG levels in cord plasma from FGR complicated pregnancies (Figure 6 D, F).

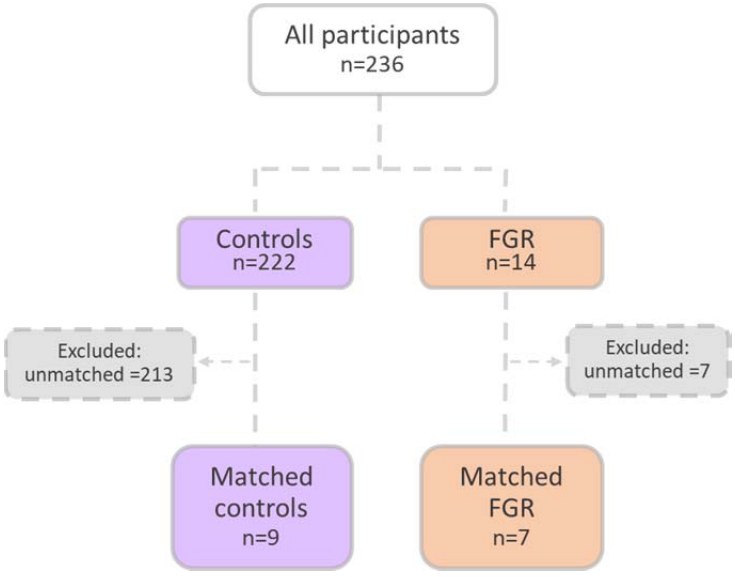

Figure 5. Patient selection flow chart. 16 Pregnant women were recruited from the Meir and Wolfson Medical Centers.

Parameter	Control *n*=9	FGR *n*=7	*P* value
Maternal age, mean ± SD, years	30.2 ± 5.6	29.14 ± 5.6	0.7291
Gestational age, mean ± SD, weeks	38.2 ± 1	37.5 ± 0.6	0.1644
Preterm delivery (<37), *n* (%)	0	0	
Pregravid BMI (kg/m^2), mean ± SD	22.8 ± 4.5	27.1 ± 3.6	0.2598
Gravidity, median (IQR)	2.3 (1.5)	2. (2)	
Parity, median (IQR)	1.2 (1.5)	1 (2)	
Maternal comorbidities, *n* (%)			
Hypertensive disorders	0	0	
Diabetes or gestational diabetes	1 (11)	1 (14)	
Asthma	0	0	
Thyroid disease	0	0	
Smoker	5	3	
Infant sex, *n* (%)			
Male	7 (77)	4 (57)	
Female	2 (23)	3 (43)	
Birthweight, mean ± SD, grams	3167 ± 494	2189.4 ± 189	***0.0004
NICU, *n* (%)	0	1 (14)	

Table 1. Clinical parameters of women included in the study. Clinical parameters did not differ among the groups, except for birthweight, which was significantly lower in the FGR group (Unpaired *t*-test, *P*=0.0004)**.**

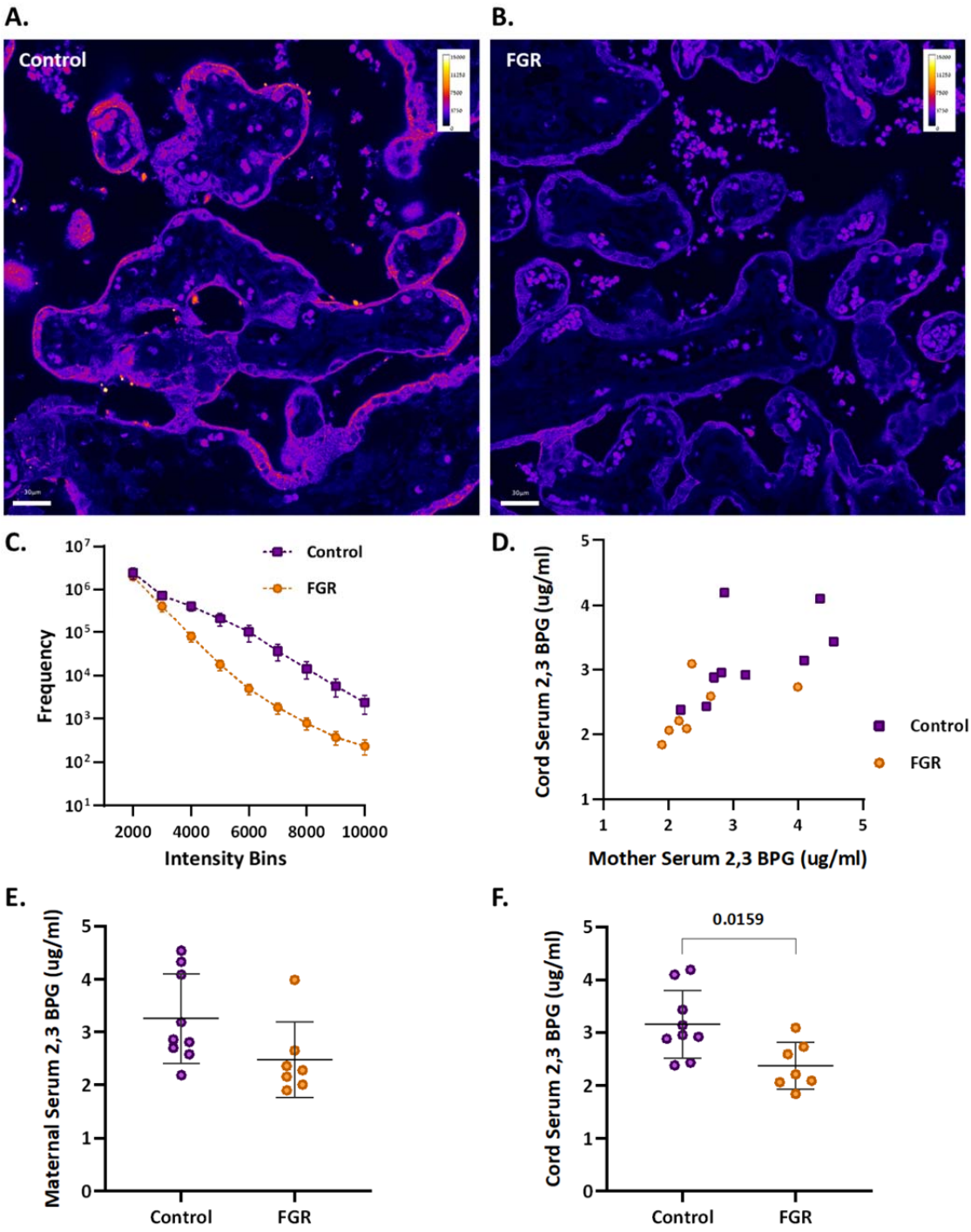

Figure 6. Human FGR placentae exhibit lower BPGM and 2,3 BPG levels. (**A, B**) Representative images of BPGM expression in control and FGR placentae. Scale bars: 30 µm. (**C**) Graph representing intensity of BPGM expression in control and FGR placentae. (**D-F**) Levels of 2,3 BPG in maternal and cord serum of control and FGR placentae. Data are from 9 control and 7 FGR women and presented as mean ± SD values. Unpaired *t* test was used for statistical analysis.

Discussion

Proper placental and fetal oxygenation is essential for a healthy pregnancy. Accordingly, maternal gestational hypoxia constitutes a risk factor for FGR incidence[34]. However, the etiology and molecular mechanism underlying idiopathic as well as maternal gestational hypoxia induced FGR remains unclear. In order to elucidate on the mechanisms leading to FGR, this study employed a murine FGR model based on maternal acute and chronic gestational hypoxia. Hypoxia-induced FGR placentae displayed smaller labyrinth fraction, higher RBC content and enlarged spiral arteries. However, *in vivo* functional MRI experiments in response to hypoxia-hyperoxia challenge are consistent with similar deoxyhemoglobin content in all groups. Oxygen release under hypoxia might be regulated by 2,3BPG, as suggested by the BPGM expression in the murine hypoxic placentae which was upregulated and concentrated in the cell side facing the maternal circulation. Conversely, human FGR placentae of unknown etiology exhibited an opposite phenotype, presenting lower BPGM expression and reduced level of 2,3 BPG in the chord serum. This suggests that induction of placenta BPGM may be part of the hypoxic adaptation response in the murine placenta; while suppression of BPGM may contribute to placenta deficiency in the human FGR.

Intra-uterine hypoxia has adverse effects on placental and embryonic development. This study shows a decreased placental and embryonal weight, and a reduction in the percent of AGA and LGA placentae and fetuses in the gestational hypoxia groups, with no difference in litter size between hypoxic and control groups. Moreover, the labyrinth area of hypoxic placentae was significantly smaller, implying an improper placental development. Previous studies showed that intermittent hypoxia increased placental weight and labyrinth size, while chronic gestational hypoxia in mice leads to reduced litter size and had no effect on the labyrinth zone[3536]. These contradictory results may be due to the different experimental setups employed in the intermittent hypoxia model, and the differences in litter size of the chronic hypoxia model, which might in turn affect placental size and development. Furthermore, the current study demonstrated an increase in the diameter of placental SpA following gestational hypoxia. This enlargement might serve as a compensational mechanism for the placental and labyrinthine size reduction, by supplying higher volumes of blood to the placenta thereby increasing oxygen content, tissue oxygenation and oxygen supply to the fetus. Previous studies have shown that gestational hypoxia from mid-late gestation increased the diameter of radial arteries compared to control[15]; however, no significant difference was observed in the spiral arteries, possibly due to the late exposure to hypoxia. However, this study mimics adaptation to early gestational

306 hypoxia and early onset placental dysfunction leading to severe FGR and therefore, might serve
307 as a better model for the human hypoxic-induced FGR.

308 MRI is an important tool for imaging changes in deoxyhemoglobin concentration *in vivo*.
309 Previous *in vivo* studies on non-treated pregnant mice obtained oxygen-hemoglobin dissociation
310 curves in mid-late gestation placentae under hyperoxia - hypoxia challenge[37]. Interestingly, in
311 the present study no significant differences were found in the R2* values between the hypoxic
312 and control placentae under hyperoxic, normoxic and hypoxic conditions. This result is
313 consistent with similar deoxyhemoglobin levels in the hypoxic and control placentae, despite the
314 upregulation of RBC levels in the hypoxic placentae. These results indicate that the partial
315 amount of HbO_2 is higher in the hypoxic placentae compared to the control, implying on the
316 ability of the placenta to maintain its oxygen levels albeit the maternal hypoxia.

317 In RBCs, the BPGM enzyme is responsible for the synthesis of 2,3 BPG, which induces the release
318 of oxygen from Hb in the mammalian organism. Remarkably, the expression of BPGM has been
319 reported in the human placental labyrinth[29], suggesting on its role in placental oxygen transfer.
320 This study shows for the first time the polar pattern of BPGM expression in both the murine and
321 human placental cells, amassing at the apical lumen, facing the maternal circulation. This polar
322 expression might increase the efficiency of oxygen sequestering from maternal blood by
323 reducing the distance between 2,3 BPG molecule and the maternal RBCs. Moreover, following
324 maternal intra-uterine hypoxia, the expression of murine placental BPGM is further upregulated,
325 suggesting a physiological role for placenta BPGM in the placental acclimatization to low oxygen
326 availability. Strikingly, attenuation in the expression of BPGM in FGR human placentae was
327 found when compared to the control. Moreover, 2,3 BPG levels in the cord serum of FGR
328 placentae were also decreased compared to control. This suggests that failure in induction of
329 placental BPGM and subsequently lower 2,3 BPG levels may contribute to the pathophysiology
330 of FGR. Remarkably, the same phenotype was observed in a murine FGR model of *igf2*+/-
331 knockout mice, where labyrinthine BPGM expression was lower compared to control dams[30].
332 This study demonstrates opposite BPGM expression patterns in mouse and human FGR,
333 suggesting that the murine FGR in our model originates in low maternal oxygen concentrations,
334 which are compensated by the placenta *via* upregulation of BPGM levels, while human FGR of
335 unknown etiology is related to a placental pathology that might include inadequate BPGM
336 expression. During human gestation, the γ hemoglobin subunit starts to decline around week 32

and β hemoglobin rises, switching from fetal to adult hemoglobin. Following this increase in HbA in the fetus, it might be possible that placental BPGM and 2,3 BPG are also used by the fetus at that stage, to mediate the release of oxygen to its organs. However, the question of how placental 2,3 BPG might be transported to the nearby maternal RBCs needs to be addressed, while a possible explanation would be a specific transport system.

In summary, we propose that placental BPGM provides an important mechanism for placental adaptation to oxygen transfer during the course of gestation. We suggest that placental BPGM sequesters oxygen from the maternal Hb, and facilitates oxygen diffusion from the maternal to the fetal circulation. These results offer a possible causative link between the expression of this enzyme and the development of an FGR. This novel molecular mechanism for the regulation of oxygen availability by the placenta might provide a better understanding of the FGR pathology and possibly pave the way toward development of novel therapies for FGR complications.

Materials and Methods

Animals

Female C57BL/6JOlaHsd mice (8-12 weeks old; Envigo, Jerusalem; n=28) were mated with C57BL/6JOlaHsd male mice (Envigo, Jerusalem; n=8). Detection of a vaginal plug the following day was considered embryonic day 0.5 (E0.5). At E0.5 or E11.5, the pregnant females were randomly allocated to control (21% O_2, n = 15) or hypoxia group (12.5% O_2, acute hypoxia; n=6, chronic hypoxia; n=7). Throughout the experiments, the animals were maintained in a temperature-controlled room (22 ± 1°C) on a 12h:12h light–dark cycle. Food and water was provided *ad libitum* and animal well-being was monitored daily. At E16.5 the pregnant females were analyzed using high-field MRI under a respiration challenge of hyperoxia-to-hypoxia (40% O_2, 20% O_2, 10% O_2). After MR imaging, the animals were sacrificed for tissue collection. All experimental protocols were approved by the Institutional Animal Care and Use Committee (IACUC) of the Weizmann Institute of Science, Protocol number: 07341021-2.

Establishment of Maternal Hypoxia Models

We applied two models of maternal hypoxia – acute and chronic. The pregnant mice were housed in a hypoxic chamber (VelO2x, Baker Ruskinn, Sanford, Maine, USA) from E11.5 (acute

hypoxia; n=6) or E0.5 (chronic hypoxia; n=7) until E16.5. On the first day in the hypoxic chamber, maternal oxygen supply was gradually reduced from 21%O_2 to 12.5 ± 0.2% O_2 by continuous infusion of a nitrogen gas. The water contained in the expired gas was trapped using silica gel beads (Merck, CAS #: 7631-86-9). A portable oxygen analyzer (PO_2-250, Lutron, Coopersburg, Pennsylvania, United States) was used to monitor the oxygen concentration in the chamber. Pregnant control females were housed in an identical chamber supplied with a constant 21% ± 0.2% O_2 concentration.

***In Vivo* MR Imaging**

MR imaging examinations were performed at a 15.2T with an MR spectrometer (BioSpec 152/11 US/R; Bruker, Karlsruhe, Germany) equipped with a gradient-coil system capable of producing pulsed gradients of 10 mT/cm in each of the three orthogonal directions. A quadrature volume coil with a 35-mm inner diameter and an homogeneous radiofrequency field of 30 mm along the axis of the magnetic field was used for both transmission and reception. Immediately prior to MR imaging, the pregnant females were anesthetized with isoflurane (3% for induction; Piramal, Mumbai, India) mixed with 2 L/min of 40% O_2 and 60% N_2 delivered into a closed induction chamber. Once anesthetized, the animals were placed in a prone position in a head holder with breathing gas mixed with isoflurane delivered through a tooth bar. Respiration rate and rectal temperature were monitored using a monitoring and gating system (Model 1030-S-50; SA Instruments, Stony Brook, NY). Respiration rate was maintained throughout the experimental period at approximately 20-30 breaths per minute by adjusting the isoflurane level (1%–2% for maintenance). Body temperature was maintained at 30±1°C (to reduce fetal movement) by adjusting the temperature of a circulating water heating blanket placed above the animal.

MR Imaging Data Acquisition

Anatomic data to determine optimal animal positioning was acquired by using a short Gradient Recalled Echo (GRE) sequence with imaging slices acquired in three orthogonal planes. The animals were positioned to maximize the number of fetuses that could be viewed while still observing maternal liver. The duration of the MRI measurements at each oxygen level was approximately 20 min. After the O_2 concentration was reduced, a 2 minute interval was given before acquiring the next set of MRI images, allowing R2* stabilization. At each oxygen phase, the nitrogen level was adjusted to maintain a constant flow of inhaled gas. To determine R2*

values three Gradient Recalled Echo (GRE) acquisitions were performed with TE= 1.6 ms, 2.6 ms and 3.6 ms. The parameters for these GRE measurements were as follows: 48 slices with slice thickness of 0.4 mm with 0.1 mm inter-slice gap, field of view 4.2 X 3.3 cm^2, pulse flip angle 40°, matrix size 280 x 220 (150 x 150 um^2 pixel size), 2 averages (motion averaging). Images were acquired with fat suppression and RF spoiling. The excitation pulse was 0.5 ms (6400 Hz bandwidth) and the acquisition bandwidth was 200 kHz. The slice order was interleaved. The sequence was respiration triggered (per slice) with an approximate TR of 800 ms.

MR Imaging Data Analysis

Images were reconstructed by Paravision 6.0 (Bruker, Karlsruhe, Germany). The GRE images used for calculating R2*s were interpolated in Matlab (MathWorks, Natick, Massachusetts, USA) to 75X75 um^2 pixel size. Regions of Interest (ROIs) were manually marked with ImageJ (U. S. National Institutes of Health, Bethesda, Maryland, USA). Subsequently, using custom written scripts all ROIs and images were imported into Matlab and the R2* for each O_2 level was determined by fitting the changes in the median signal intensity of each ROI to a single exponential decay [Eq 1]:

$$Int = Int_0 \cdot e^{-R_2^* \cdot TE} \quad \text{[Equation 1]}$$

Tissue collection

Mouse placentae samples: After MR Imaging of the animals, maternal blood was collected from the submandibular vein, followed by cervical dislocation. Maternal hematocrit and Hb levels were determined using i-STAT CG8+ cartridge (Abbott, Cat. No. ABAXIS-600-9001-10, Chicago, Illinois, USA). Uterine tissues were immersed in PBS to count the number of fetuses and resorptions. Fetuses and placentae were immediately removed and weighed, following by fixation in 4% paraformaldehyde. Grade of embryonic and placental weight was classified as SGA (weight less than the 10^{th} percentile), large for gestational age (LGA, weight greater than the 90^{th} percentile), and appropriate for gestational age (AGA, weight between the 10^{th} and 90^{th} percentiles).

Human placentae samples: The study was approved by the Meir and Wolfson Medical Center IRB Local Committee (Protocols: # 0147-20 MMC and #185-19-WOMC). Written informed consent was obtained from all participants prior to delivery. Placentae from 9 healthy uncomplicated pregnancies and from 7 pregnancies complicated by fetal growth restriction

(FGR) were collected immediately after elective cesarean deliveries. Two biopsies were taken from each placenta, one from a peripheral and one from a central lobule. The biopsied material (~ 1 cm^3) was immediately fixed in formalin. FGR birth weight standards were based on the Dollberg curve.

Human Serum: Maternal and cord serum samples were collected from the enrolled patients prior to delivery, and from the umbilical cord just following delivery. The umbilical cord was wiped clean and blood was drawn from the vein. Blood samples were centrifuged (1000g, 10 minutes at room temperature), and serum aliquots were stored at –80°C in dedicated tubes for analyses at the Weizmann Institute.

Immunohistochemistry and Microscopy

Fixed murine and human placentae were processed and embedded in paraffin. Representative 5 µm sections were taken from each tissue and used for immunohistochemistry (IHC).

All slides were dewaxed and rehydrated in xylene and a series of ethanol washes. IHC staining involved antigen retrieval in a pressure cooker using citrate buffer (pH=6) and blocking of non-specific binding with 20% NHS and 0.2% Triton in PBS. Slides were incubated with polyclonal rabbit primary anti-BPGM antibody (1:200, Sigma-Aldrich, Cat. No. HPA016493, RRID:AB_1845414), followed by incubation with an HRP anti-Rabbit secondary antibody (1:100, Jackson ImmunoResearch Labs, Cat# 111-035-003, RRID:AB_2313567) followed by Opal 690 (1:500, Akoya Biosciences, Cat. No. FP1497001KT). Negative controls for each immunostaining were incubated with secondary antibody only.

Images were captured using Nikon Eclipse Ti2_E microscope, Yokogawa CSU W1 spinning disk, photometrics Prime 25B camera with NIS elements AR 5.11.01 64bit software.

Placental Morphological Analysis

For the assessment of placental labyrinth size, fractional area expressing both BPGM and containing fetal RBCs of each placenta was computed *via* use of the color thresholding and area fraction tools in ImageJ. Approximately 10 measurements were made per each placenta. Spiral arteries diameter was measured manually using ImageJ, namely, for each spiral artery 5-6 measurements were made. For the assessment of RBC levels in the labyrinth, thresholding of the RBC auto fluorescence signal was employed. Quantification of mouse placental BPGM in the

labyrinth was performed using color thresholding in ImageJ, 10 identical measurements were done for each placenta, 500x500 µm each. For the assessment of BPGM in the SpA TGCs, regions of interest were drawn manually implying the same thickness from the inner vessel border followed by color thresholding in ImageJ. We quantified human BPGM expression level by creating a binned intensity histogram of all the pixels expressing BPGM signal above a minimal background value (of 1000), in a single slice of each sample using Fiji Macro[38]. As red blood cells (RBC) have high auto fluorescence in all channels, we discarded RBC regions them prior BPGM quantification. This is done in Imaris (Oxford company) by creating Surface object for RBC (default parameters, automated absolute intensity threshold), and using it to create new PBGM channel in which the values in the RBC regions are set to zero.

LC–MS/MS measurement of 2,3-BPG

Ten-uL aliquots of plasma were extracted with 80uL of extraction buffer (10mM ammonium acetate/5mM ammonium bicarbonate, pH 7.7 and methanol in ratio 1:3 by volume), and 10uL of methionine sulfone (1ug/mL in water) was added as internal standard. The mixture was vortexed, incubated at 10°C for 10min, then centrifuged (21,000g for 10min). The supernatant was collected for consequent LC–MS/MS analysis. The LC–MS/MS instrument consisting of an Acquity I-class UPLC system (Waters) and Xevo TQ-S triple quadrupole mass spectrometer (Waters), equipped with an electrospray ion source, was used for analysis of 2,3-BPG. MassLynx and TargetLynx software (v.4.1, Waters) were applied for the acquisition and analysis of data. Chromatographic separation was performed on a 150mm × 2.1mm internal diameter, 1.7-µm BEH Z-HILIC column (Waters Atlantis Premier) with mobile phases A (20mM ammonium carbonate, pH 9.25/acetonitrile, 80/20 by volume) and B (acetonitrile) at a flow rate of 0.4ml min−1 and column temperature of 25°C. A gradient was used as follows: for 0–0.8min a linear decrease from 80 to 35%B, for 0.8–5.6min further decrease to 25%B, for 5.6–6.0min hold on 25%B, then for 6.0-6.4min back to 80%B, and equilibration at 80%B for 2.6min. Samples kept at 8°C were automatically injected in a volume of 5µl. 2,3-BPG concentration was calculated using a standard curve, ranging from 0.1–100µg ml−1. For MS detection MRM transitions 265.0>78.8, 265.0>167.0 m/z (ESI -) were applied in case of 2,3-BPG, with collision energies 31 and 12eV, respectively. Internal standard was detected using MRM 182.1>56.0 m/z (ESI +), with collision energy 18eV.

Statistical Analysis

Ordinary one-way Anova test was applied for the comparison between the three pregnant females groups (control, acute and chronic hypoxia). Litter means were used for statistical analysis of fetal and placental weights. Unpaired *t*-test was used for the analysis of the IF images of FGR and control human placentae. The data were considered to indicate a significant difference when *P* values were less than 0.05. All results are represented as the mean ± SD. Statistical analysis was performed using Graphpad Prism 6 (GraphPad Software, San Diego, USA) for Windows.

Acknowledgements

This work was supported by the Weizmann - Ichilov (Tel Aviv Sourasky Medical Center) Collaborative Grant in Biomedical Research (to MN) and by the Israel Science Foundation KillCorona grant 3777/19 (to MN, MK). Graphical abstract was created with BioRender.com.

Author contributions and disclosures

S.S., N.D., M.N. designed the research, S.S., T.H., L.F.A, L.B.M., A.B., T.M., performed the research, L.F.A., R.P.M., M.K., T.B.S, contributed vital new reagents or analytical tools, S.S, T.H., O.G., analyzed the data, and S.S., N.D. and M.N. wrote the paper.

Conflict-of-Interest

The authors declare no conflicts of interest.

Data availability

All data are available, without restriction, upon request.

References

1. Gude NM, Roberts CT, Kalionis B, King RG. Growth and function of the normal human placenta. *Thromb Res*. 2004;114(5-6 SPEC. ISS.):397-407. doi:10.1016/j.thromres.2004.06.038

2. Garnica AD, Chan WY. The role of the placenta in fetal nutrition and growth. *J Am Coll Nutr*. 1996;15(3):206-222. doi:10.1080/07315724.1996.10718591

3. Burton GJ, Fowden AL. The placenta: A multifaceted, transient organ. *Philos Trans R Soc B Biol Sci*. 2015;370(1663). doi:10.1098/RSTB.2014.0066

4. Woods L, Perez-Garcia V, Hemberger M. Regulation of Placental Development and Its Impact on Fetal Growth—New Insights From Mouse Models. *Front Endocrinol (Lausanne)*. Published online 2018. doi:10.3389/fendo.2018.00570

5. Sun C, Groom KM, Oyston C, Chamley LW, Clark AR, James JL. The placenta in fetal growth restriction: What is going wrong? *Placenta*. 2020;96:10-18. doi:10.1016/J.PLACENTA.2020.05.003

6. Romo A, Carceller R, Tobajas J. Intrauterine Growth Retardation (IUGR): Epidemiology and Etiology. *Abstr Ref Ped Endocrinol Rev*. 2008;6:pp.

7. Lausman A, Kingdom J, Gagnon R, et al. Intrauterine growth restriction: Screening, diagnosis, and management. *J Obstet Gynaecol Canada*. 2013;35(8):749-757. doi:10.1016/S1701-2163(15)30866-5

8. Sharma D, Shastri S, Sharma P. Intrauterine Growth Restriction: Antenatal and Postnatal Aspects. Clin Med Insights Pediatr. 2016;10:67. doi:10.4137/CMPED.S40070

9. Von Beckerath AK, Kollmann M, Rotky-Fast C, Karpf E, Lang U, Klaritsch P. Perinatal complications and long-term neurodevelopmental outcome of infants with intrauterine growth restriction. *Am J Obstet Gynecol*. 2013;208(2):130.e1-130.e6. doi:10.1016/J.AJOG.2012.11.014

10. Chew LC, Verma RP. Fetal Growth Restriction. In: StatPearls. Treasure Island (FL): StatPearls Publishing; June 11, 2022.

11. Ghidini A. Idiopathic fetal growth restriction: A pathophysiologic approach. *Obstet Gynecol Surv*. 1996;51(6):376-382. doi:10.1097/00006254-199606000-00023

12. Burton GJ. Oxygen, the Janus gas; its effects on human placental development and function. In: *Journal of Anatomy*. ; 2009. doi:10.1111/j.1469-7580.2008.00978.x

13. Carter AM. Placental gas exchange and the oxygen supply to the fetus. *Compr Physiol*. Published online 2015. doi:10.1002/cphy.c140073

14. Zhou J, Xiao D, Hu Y, et al. Gestational hypoxia induces preeclampsia-like symptoms via heightened endothelin-1 signaling in pregnant rats. *Hypertension*. 2013;62(3):599-607. doi:10.1161/HYPERTENSIONAHA.113.01449

15. Cahill LS, Rennie MY, Hoggarth J, et al. Feto- and utero-placental vascular adaptations to chronic maternal hypoxia in the mouse. *J Physiol*. 2018;596(15):3285-3297.

doi:10.1113/JP274845

16. Higgins JS, Vaughan OR, Fernandez de Liger E, Fowden AL, Sferruzzi-Perri AN. Placental phenotype and resource allocation to fetal growth are modified by the timing and degree of hypoxia during mouse pregnancy. *J Physiol*. 2016;594(5):1341-1356. doi:10.1113/JP271057

17. Tomlinson TM, Garbow JR, Anderson JR, Engelbach JA, Nelson DM, Sadovsky Y. Magnetic resonance imaging of hypoxic injury to the murine placenta. Am J Physiol - Regul Integr Comp Physiol. 2010;298(2):312-319. doi:10.1152/ajpregu.00425.2009

18. Howard RB, Hosokawa T, Maguire MH. Hypoxia-induced fetoplacental vasoconstriction in perfused human placental cotyledons. *Am J Obstet Gynecol*. 1987;157(5):1261-1266. doi:10.1016/S0002-9378(87)80307-1

19. Mairbäurl H, Weber RE. Oxygen Transport by Hemoglobin. Published online 2012. doi:10.1002/cphy.c080113

20. Avni R, Neeman M, Garbow JR. Functional MRI of the placenta – From rodents to humans. *Placenta*. 2015;36(6):615-622. doi:10.1016/J.PLACENTA.2015.04.003

21. Avni R, Golani O, Akselrod-Ballin A, et al. MR Imaging–derived Oxygen-Hemoglobin Dissociation Curves and Fetal-Placental Oxygen-Hemoglobin Affinities. *Radiology*. 2016;280(1):68-77. doi:10.1148/radiol.2015150721

22. Sasaki R, Ikura K, Narita H, Yanagawa S ichi, Chiba H. 2,3-bisphosphoglycerate in erythroid cells. *Trends Biochem Sci*. 1982;7(4):140-142. doi:10.1016/0968-0004(82)90205-5

23. Mulquiney PJ, Kuchel PW. Model of 2,3-bisphosphoglycerate metabolism in the human erythrocyte based on detailed enzyme kinetic equations: equations and parameter refinement. Biochem J. 1999;342 Pt 3(Pt 3):581-596.

24. Steinberg MH, Benz EJ, Adewoye AH, Ebert BL. Pathobiology of the Human Erythrocyte and Its Hemoglobins. *Hematol Basic Princ Pract*. Published online 2018:447-457. doi:10.1016/B978-0-323-35762-3.00033-0

25. Bauer DE, Kamran SC, Orkin SH. Reawakening fetal hemoglobin: prospects for new therapies for the-globin disorders. Published online 2012. doi:10.1182/blood

26. Bauer C, Ludwig I, Ludwig M. Different effects of 2.3 diphosphoglycerate and adenosine triphosphate on the oxygen affinity of adult and foetal human haemoglobin. *Life Sci*. 1968;7(23):1339-1343. doi:10.1016/0024-3205(68)90249-X

27. Frier JA, Perutz MF. Structure of human foetal deoxyhaemoglobin. *J Mol Biol*. 1977;112(1):97-112. doi:10.1016/S0022-2836(77)80158-7

28. Adachi K, Konitzer P, Pang J, Reddy KS, Surrey S. Amino Acids Responsible for Decreased 2, 3-Biphosphosphoglycerate Binding to Fetal Hemoglobin. *Blood*. 1997;90(8):2916-2920. doi:10.1182/BLOOD.V90.8.2916

29. Pritlove DC, Gu M, Boyd CAR, Randeva HS, Vatish M. Novel Placental Expression of 2,3-Bisphosphoglycerate Mutase. *Placenta*. 2006;27(8):924-927.

589 doi:10.1016/j.placenta.2005.08.010

590 30. Gu M, Pritlove DC, Boyd CAR, Vatish M. Placental Expression of 2,3 Bisphosphoglycerate
591 Mutase in IGF-II Knock out Mouse: Correlation of Circulating Maternal 2,3
592 Bisphosphoglycerate and Fetal Growth. *Placenta*. 2009;30(10):919-922.
593 doi:10.1016/j.placenta.2009.08.005

594 31. Keyes LE, Armaza JF, Niermeyer S, Vargas E, Young DA, Moore LG. Intrauterine Growth
595 Restriction, Preeclampsia, and Intrauterine Mortality at High Altitude in Bolivia. *Pediatr*
596 *Res 2003 541*. 2003;54(1):20-25. doi:10.1203/01.pdr.0000069846.64389.dc

597 32. Jang EA, Longo LD, Goyal R. Antenatal maternal hypoxia: Criterion for fetal growth
598 restriction in rodents. *Front Physiol*. 2015;6(MAY):176.
599 doi:10.3389/FPHYS.2015.00176/BIBTEX

600 33. Faura J, Ramos J, Reynafarje C, English E, Finne P, Finch CA. Effect of Altitude on
601 Erythropoiesis. *Blood*. 1969;33(5):668-676. doi:10.1182/BLOOD.V33.5.668.668

602 34. Ducsay CA, Goyal R, Pearce WJ, Wilson S, Hu XQ, Zhang L. Gestational hypoxia and
603 developmental plasticity. Physiol Rev. 2018;98(3):1241-1334. doi:
604 10.1152/physrev.00043.2017

605 35. Matheson H, Veerbeek JHW, Charnock-Jones DS, Burton GJ, Yung HW. Morphological
606 and molecular changes in the murine placenta exposed to normobaric hypoxia
607 throughout pregnancy. *J Physiol*. 2016;594(5):1371-1388. doi:10.1113/JP271073

608 36. Badran M, Abuyassin B, Ayas N, Laher I. Intermittent hypoxia impairs uterine artery
609 function in pregnant mice. *J Physiol*. 2019;597(10):2639-2650. doi:10.1113/JP277775

610 37. Avni R, Golani O, Akselrod-Ballin A, et al. MR Imaging–derived Oxygen-Hemoglobin
611 Dissociation Curves and Fetal-Placental Oxygen-Hemoglobin Affinities. *Radiology*.
612 2016;000(0):150721. doi:10.1148/radiol.2015150721

613 38. Schindelin J, Arganda-Carreras I, Frise E, et al. Fiji: An open-source platform for biological-
614 image analysis. *Nat Methods*. 2012;9(7):676-682. doi:10.1038/NMETH.2019

615

616

617

618

619

620

621

622

623

624

Supplementary

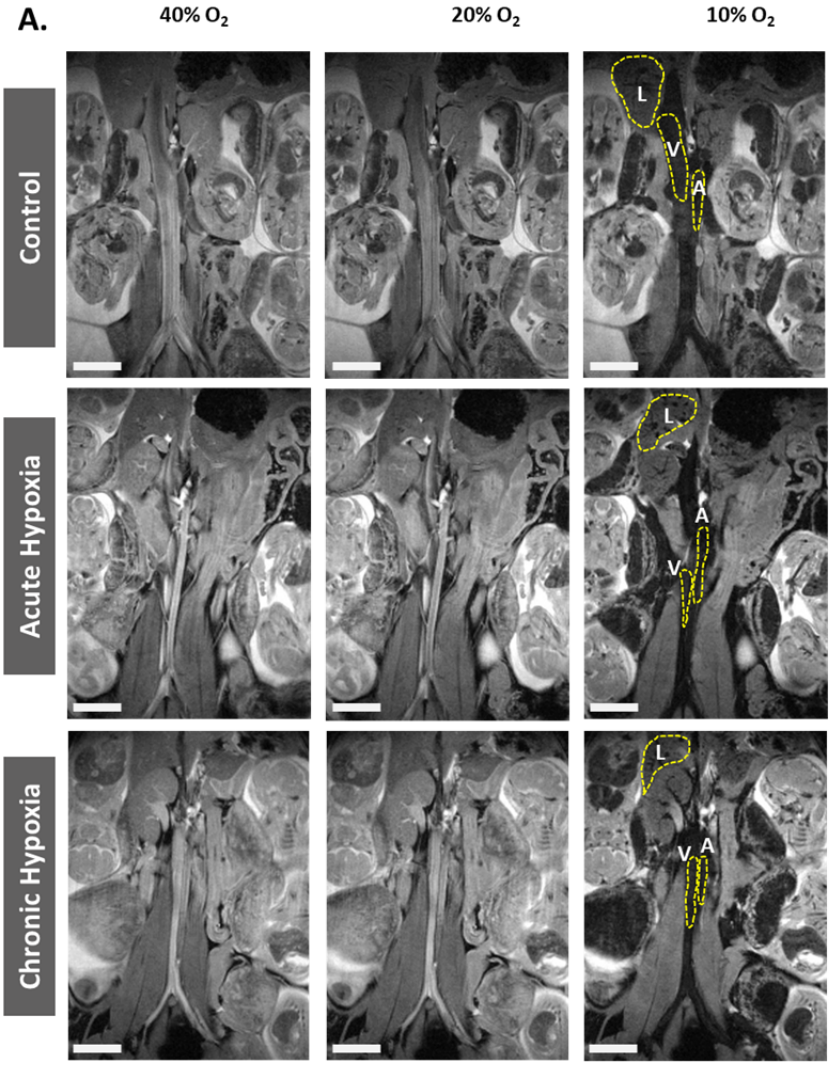

Figure S1. Effects of maternal hypoxia during gestation on R2* values following hyperoxia-hypoxia challenge. (**A**) Representative R2* images of control and hypoxic chamber group show several dams and their liver (L), aorta (A) and vena cava (V). Scale bars: 0.5 cm.

MR imaging of mother, embryos and placentae

Video 1, 2, 3: Representative MRI scan videos of control. acute and chronic hypoxia dams respectively.

Mother

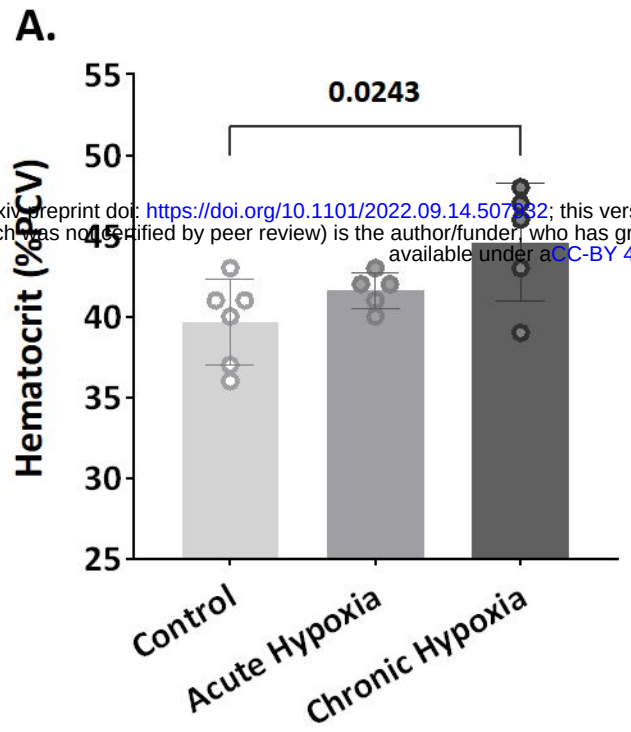

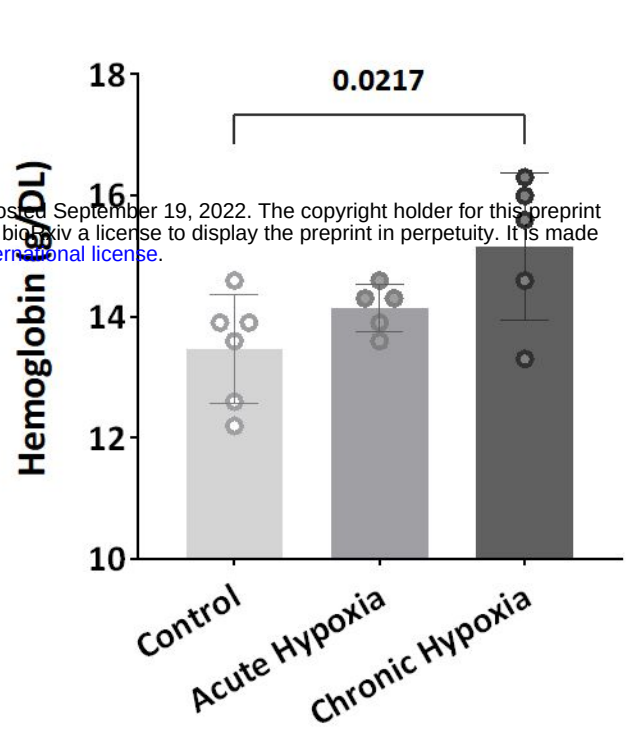

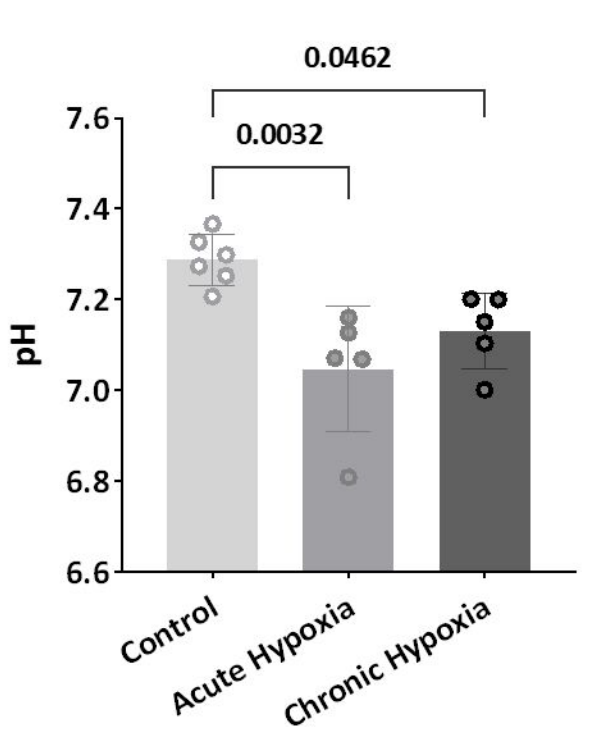

Fetus and placenta

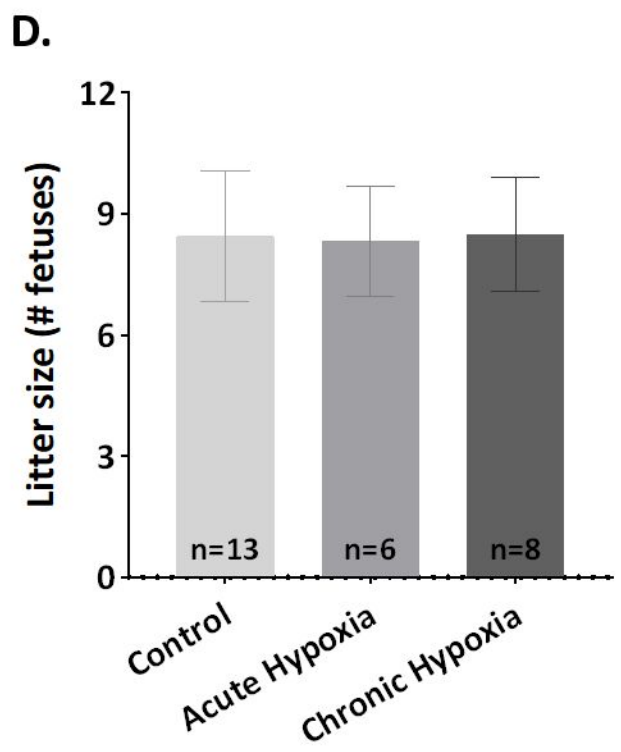

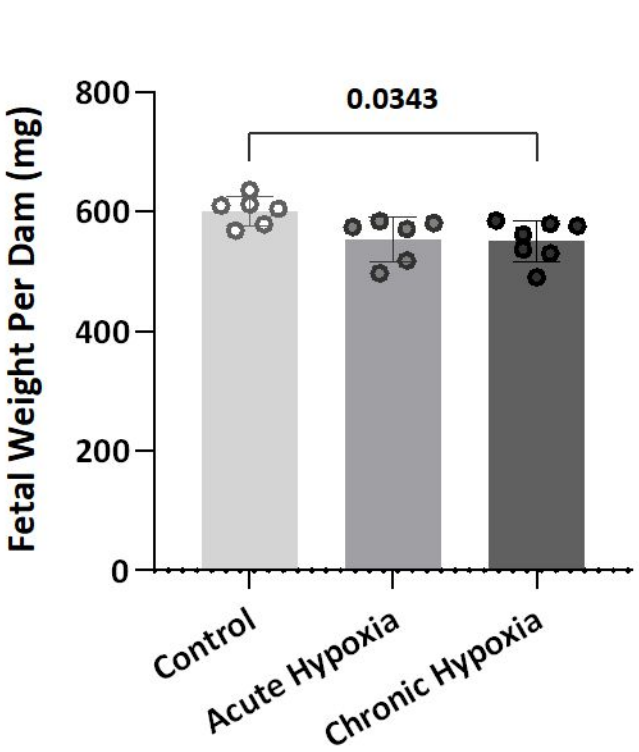

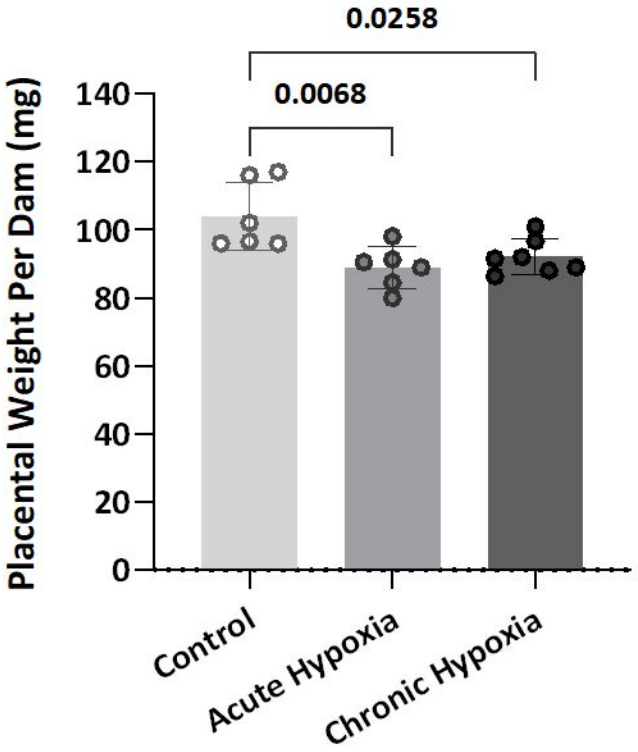

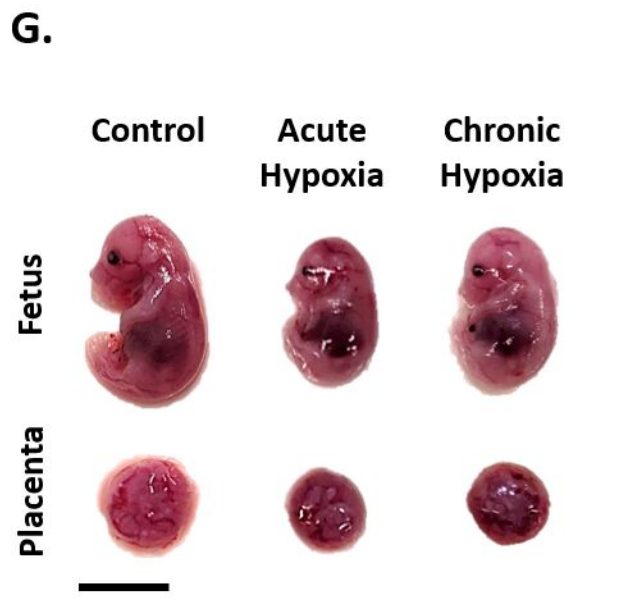

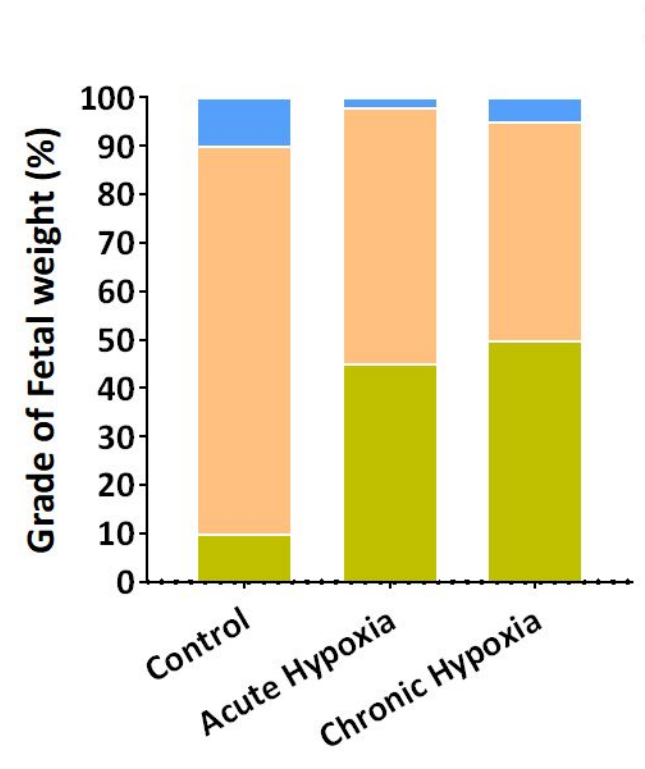

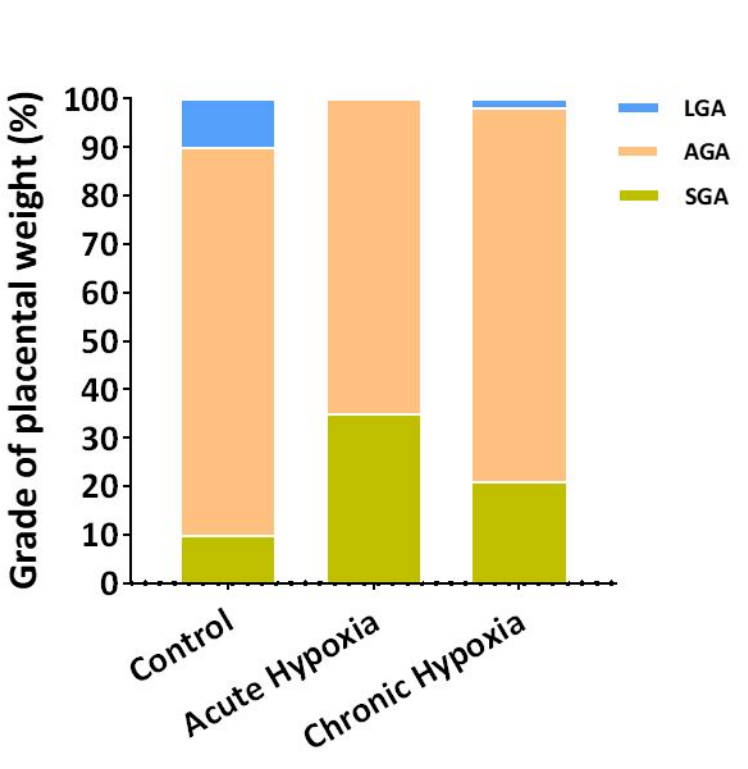

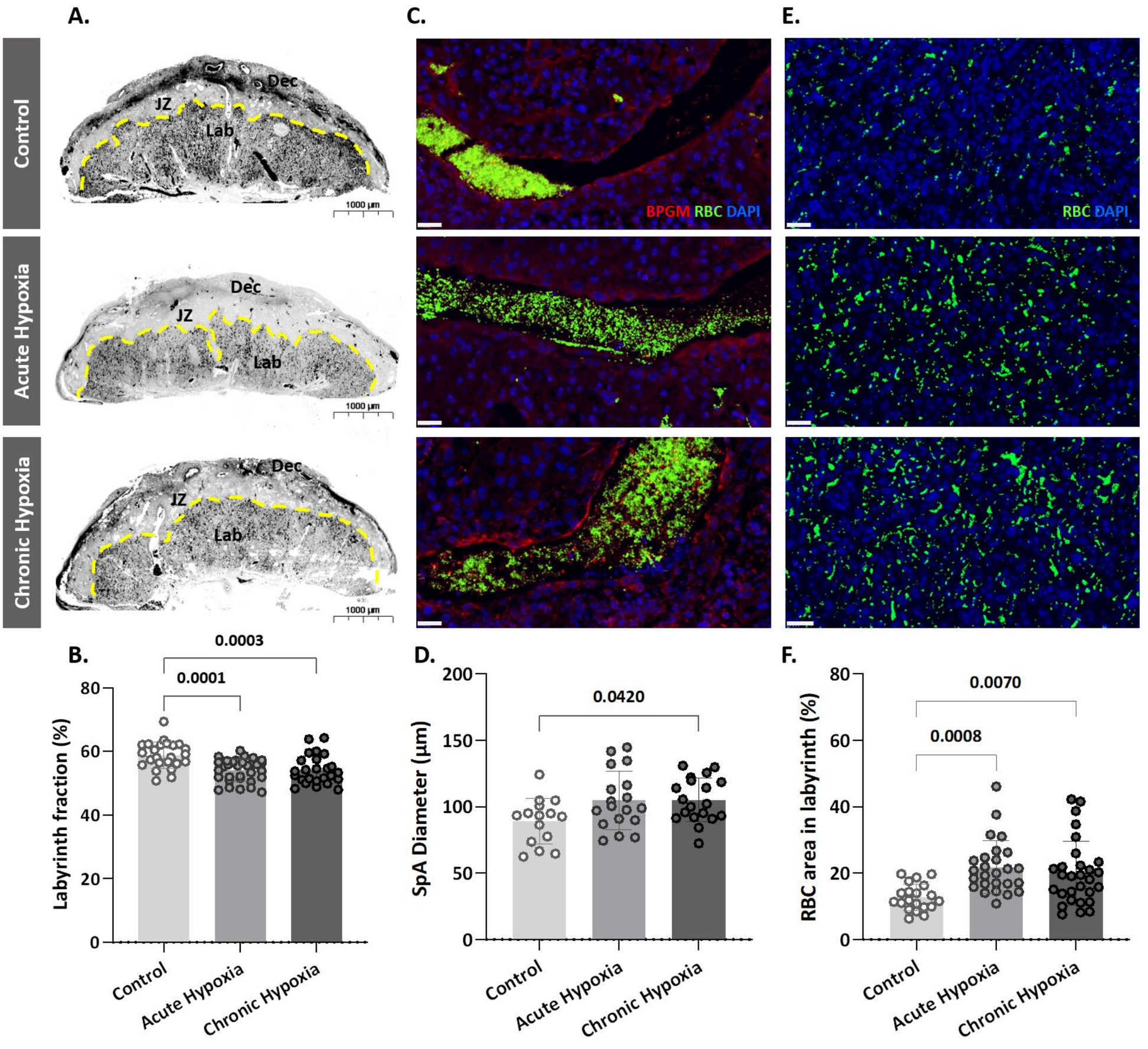
A.
C.
E.
Control
Acute Hypoxia
Chronic Hypoxia
Dec
JZ
Lab
1000 µm
BPGM RBC DAPI
RBC DAPI
B.
0.0003
0.0001
Labyrinth fraction (%)
80
60
40
20
0
Control
Acute Hypoxia
Chronic Hypoxia
D.
0.0420
SpA Diameter (µm)
200
150
100
50
0
F.
0.0070
0.0008
RBC area in labyrinth (%)

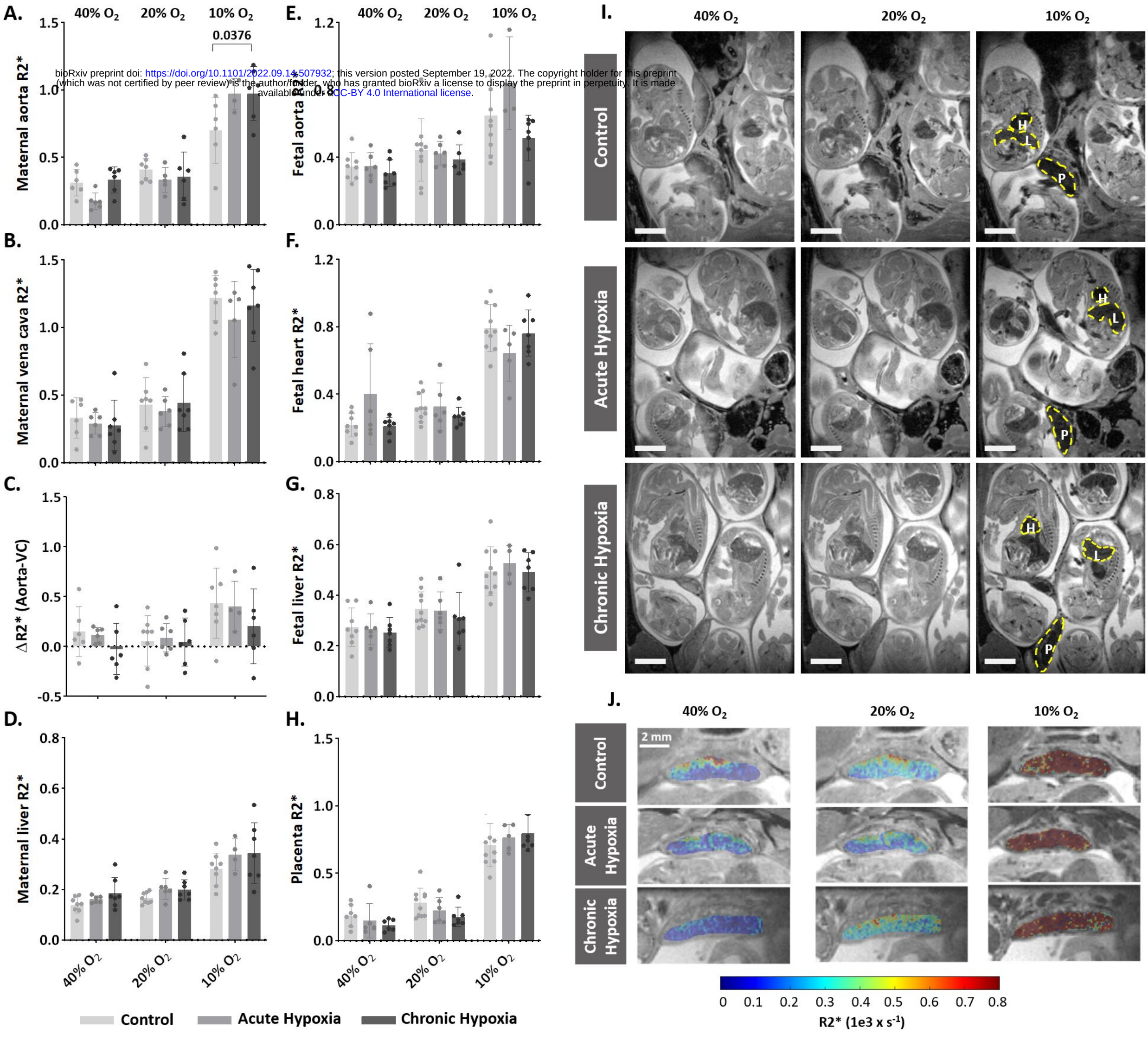

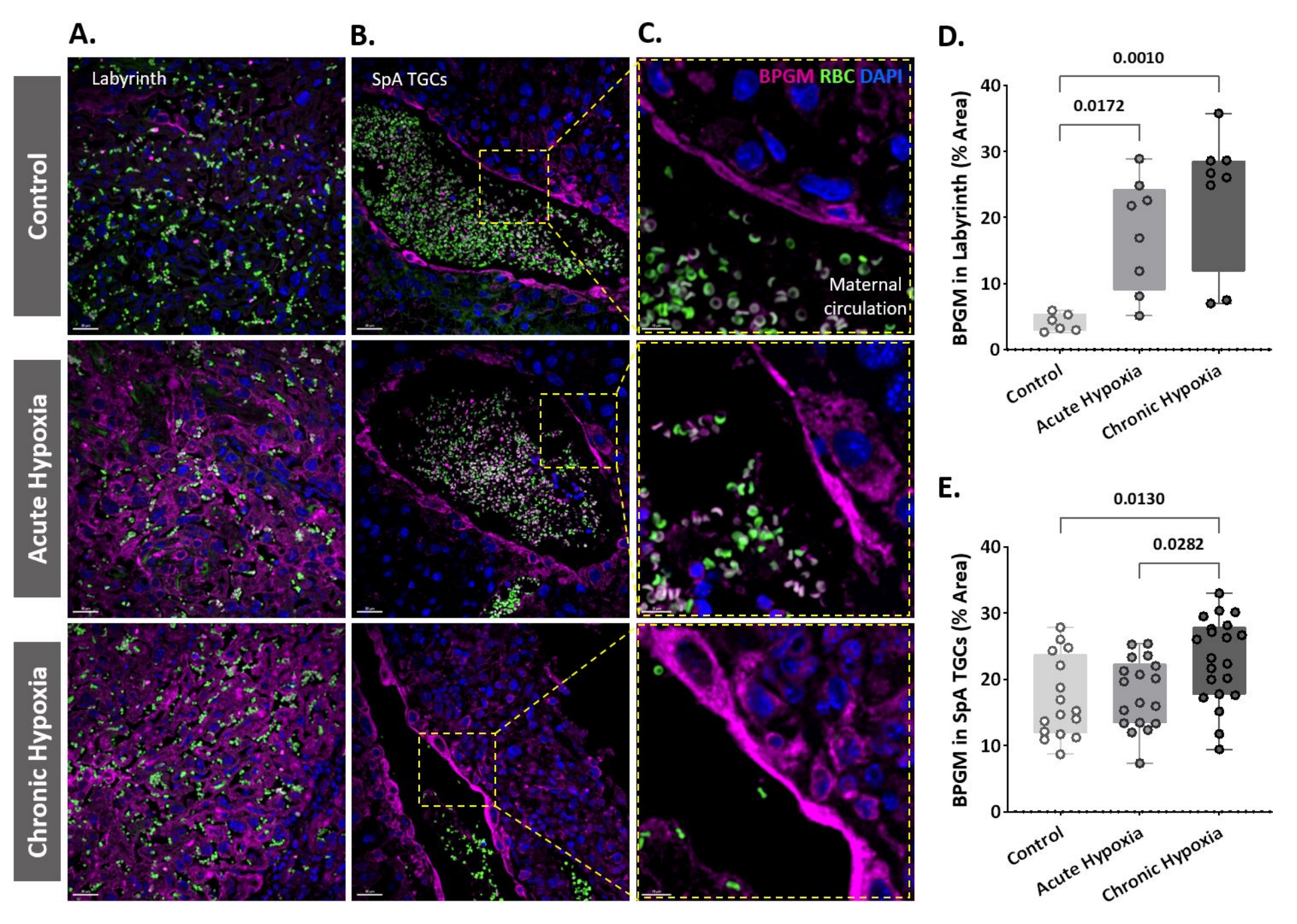
A.
B.
C.
D.
E.
Control
Acute Hypoxia
Chronic Hypoxia
Labyrinth
SpA TGCs
BPGM RBC DAPI
Maternal circulation
0.0010
0.0172
BPGM in Labyrinth (% Area)
0
10
20
30
40
Control
Acute Hypoxia
Chronic Hypoxia
0.0130
0.0282
BPGM in SpA TGCs (% Area)
0
10
20
30
40
Control
Acute Hypoxia
Chronic Hypoxia

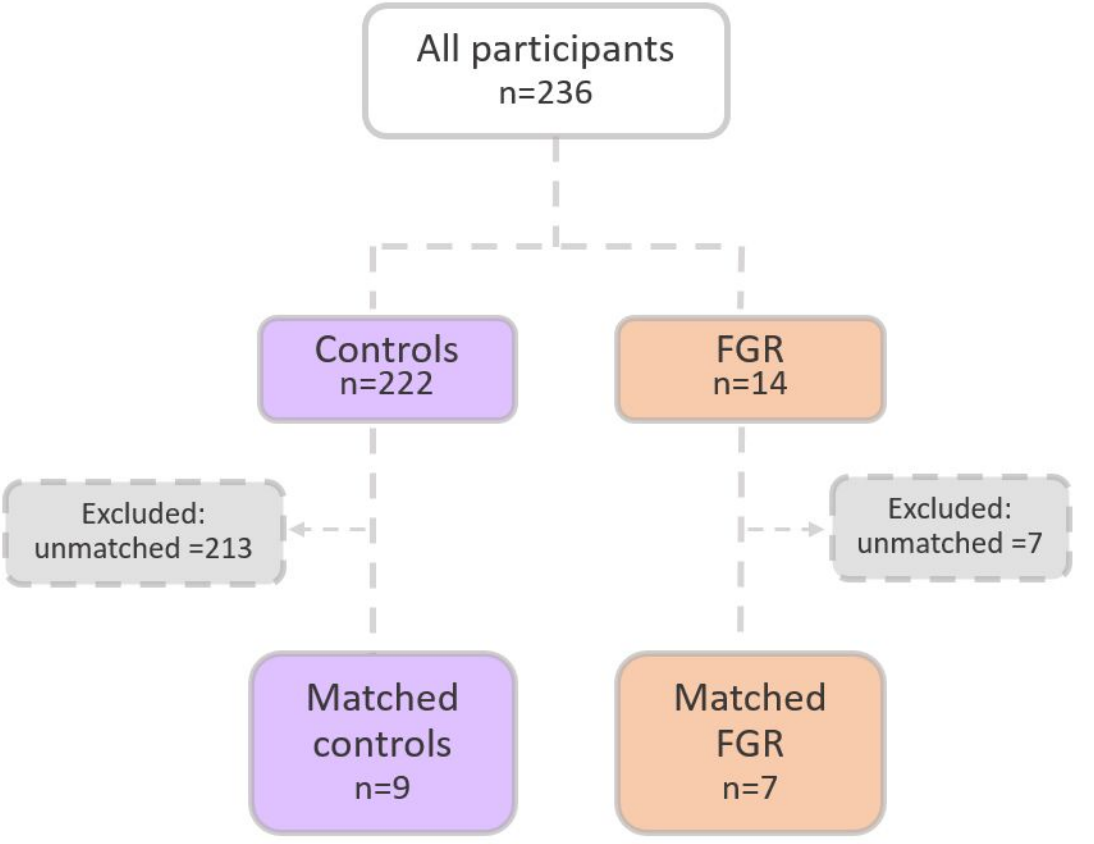
All participants
n=236
Controls
n=222
FGR
n=14
Excluded:
unmatched =213
Excluded:
unmatched =7
Matched
controls
n=9
Matched
FGR
n=7

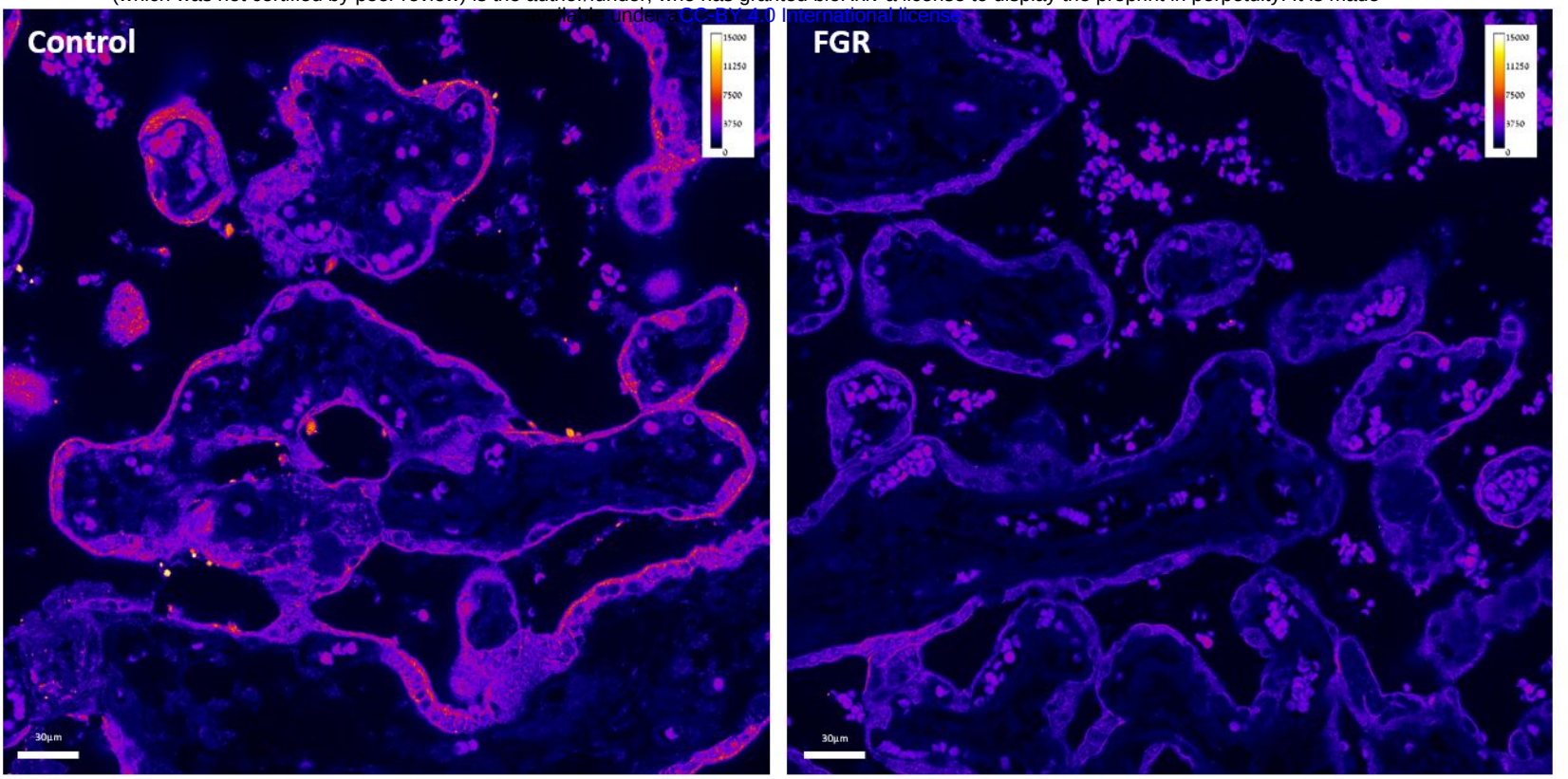

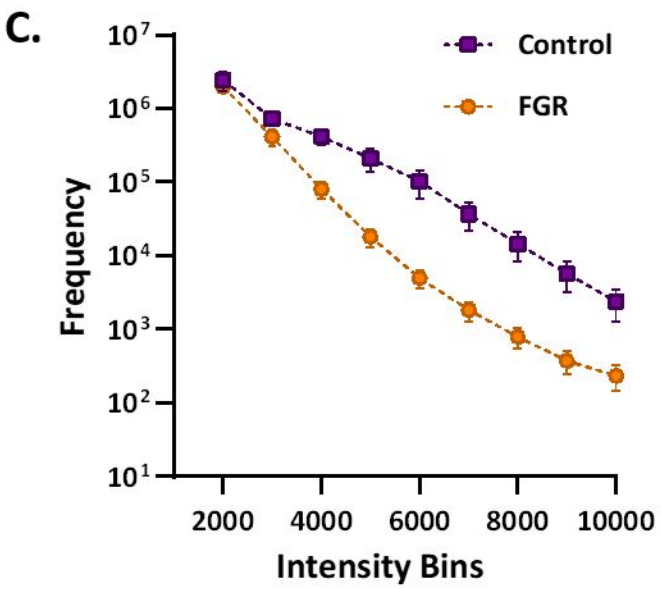

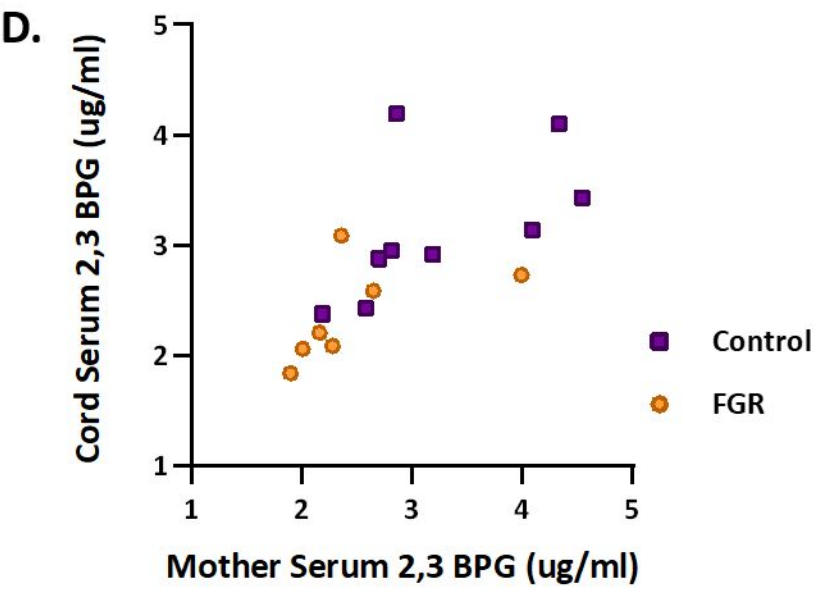

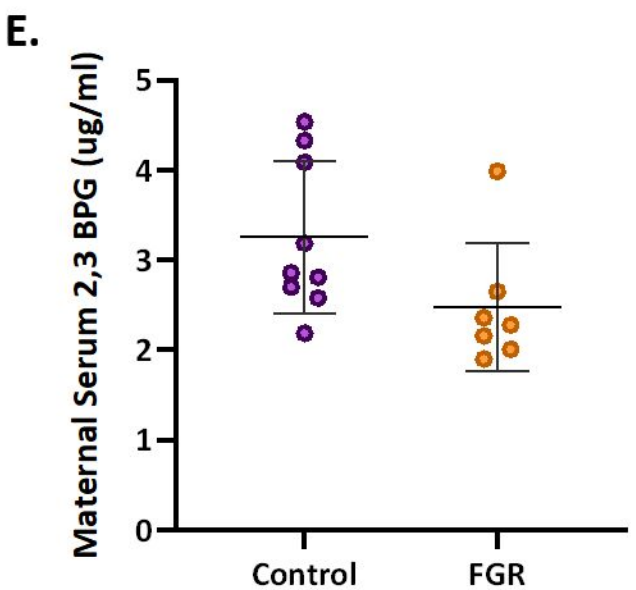

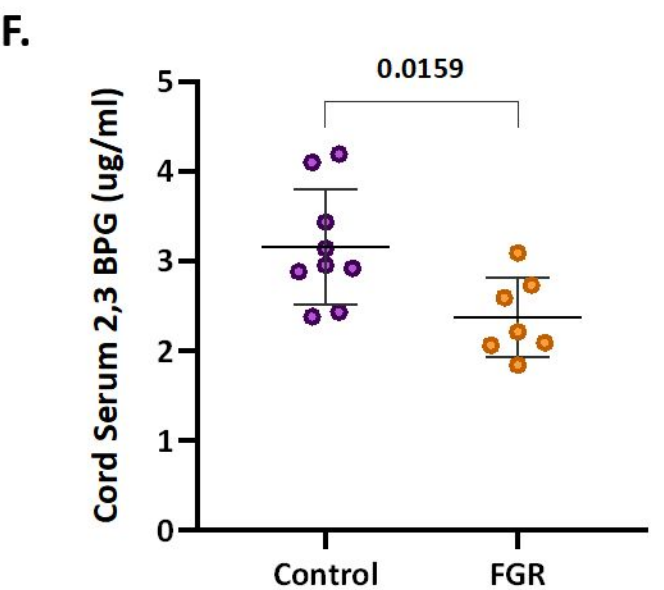

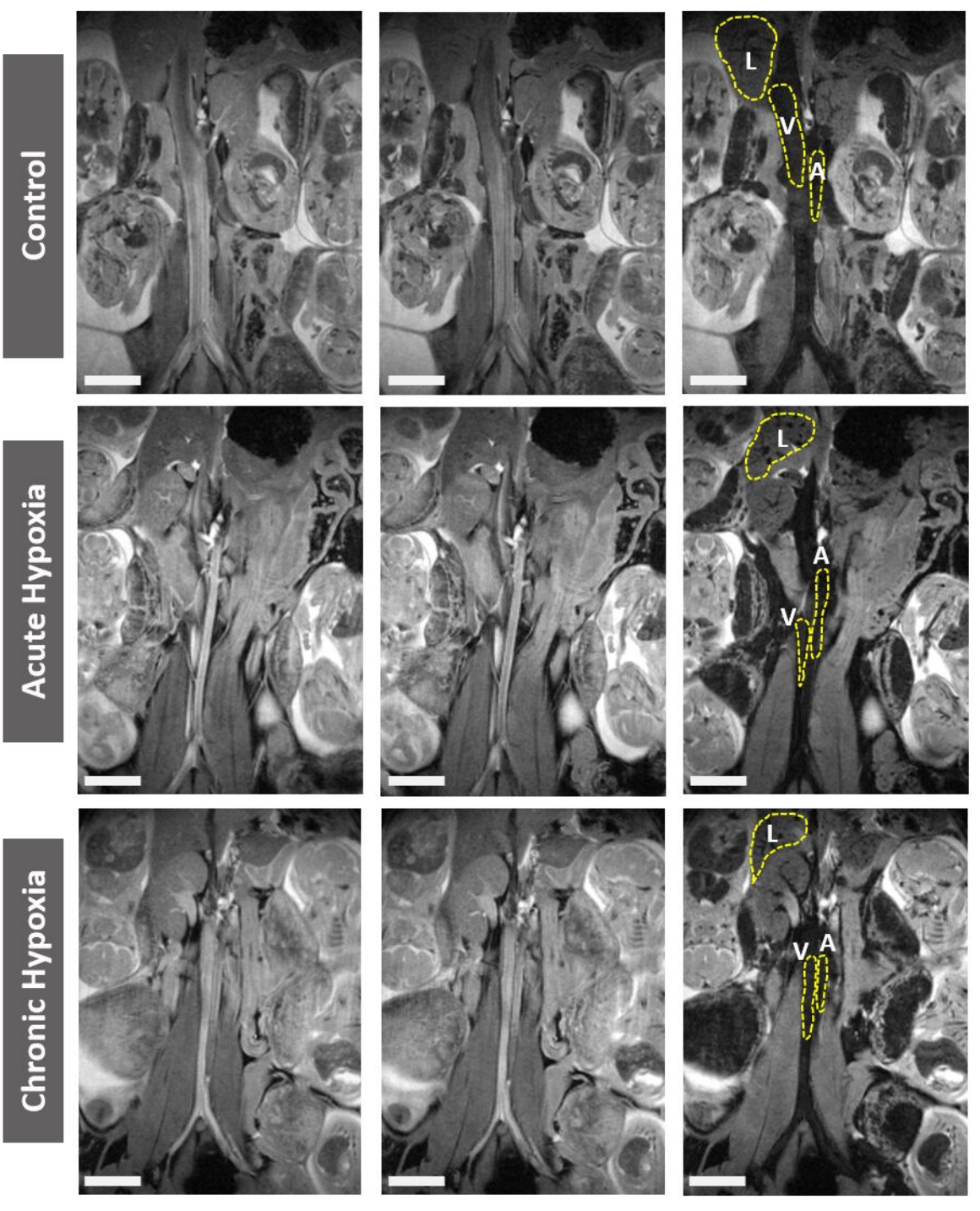
40% O_2
20% O_2
10% O_2
Control
Acute Hypoxia
Chronic Hypoxia
L
V
A
L
A
V
L
V
A